Manuscript

Click here to view linked References

Click here to access/download;Manuscript;Text_Mas-et-al_JIG_Rev.doc

COASTAL WETLANDS AS MARKERS OF TRANSGRESSION IN PROXIMAL EXTENSIONAL SYSTEMS (BERRISASIAN, W CAMEROS BASIN, SPAIN)

Authors:

Ramón Mas[1, 3], Mª Eugenia Arribas[2, †], Laura González-Acebrón[1], I. Emma Quijada[4], Sonia Campos-Soto[1, 3], Pablo Suarez-Gonzalez[5], Sara Sacristán-Horcajada[1], José Arribas[2, 3], M. Isabel Benito[1, 3], Carlos Pérez-Garrido[2], Ángela Alonso[*6].

Addresses:

[1.] *Departamento de Geodinámica, Estratigrafía y Paleontología, Universidad Complutense de Madrid, C/ José Antonio Nováis 12, 28040 Madrid, Spain.*

[2.] *Departamento de Mineralogía y Petrología Universidad Complutense de Madrid, C/ José Antonio Nováis 12, 28040 Madrid, Spain.*

[3.] *Instituto de Geociencias IGEO (CSIC, UCM), C/ Severo Ochoa 7, Ciudad Universitaria, 28040 Madrid, Spain.*

[4.] *Departamento de Geología, Universidad de Oviedo, C/ Jesús Arias de Velasco s/n, 33005 Oviedo, Spain*

[5.] *Área de Geología, Universidad Rey Juan Carlos, C/ Tulipán s/n, Móstoles, Spain.*

[6.] *Retired. Department of Navigation and Earth Sciences. University of A Coruña, A Coruña, Spain*

† Corresponding Author: Tel.: +34913944918. Fax: +34915442535.

Email: earribas@geo.ucm.es

ABSTRACT

The early stages of intraplate extensional systems commonly are recorded by deposition of continental sediments. In this context, given appropriate tectonics and eustasy, transgressions can be well recorded in the areas of the basins located close to the sea, but they may be difficult to recognize in the innermost landwards areas of the system. This situation occurs in the innermost Upper Jurassic-Early Cretaceous Cameros Basin, part of the Iberian Extensional System (N. Spain), where a Berriasian transgression is recorded. The Berriasian succession in this area consists of siliciclastic deposits (sandstone and mudstone) of the Salcedal Formation and of carbonate and mixed carbonate-fine siliciclastic deposits (limestone and marl) of the San Marcos Formation. The sedimentological analysis of this depositional succession indicates that a Berriasian carbonate coastal wetland system occupied that sector of the Cameros Basin during deposition of the San Marcos Formation. This carbonate coastal wetland system consisted of shallow and quiet water bodies including some with marine influence others with no to very little marine influence, and palustrine areas. A semiarid climate characterized by the seasonal alternation of short wet and long dry periods caused water bodies of the system to undergo episodic desiccation and subaerial exposure. Moreover, this complex mosaic of sub-environments was connected laterally with a distal zone of a distributive fluvial system that was rimmed by siliciclastic tidal flats during phases of greater marine influence.

The paleogeographic arrangement of this coastal wetland depositional system indicates that the marine influence came from the Basque-Cantabrian Basin to the north. During the period of Berriasian maximum marine influence, accommodation linked to the eustatic rise added to accommodation generated by tectonic subsidence from the extensional reactivation of late Variscan strike-slip faults. All these factors favored marine incursion into the west Cameros Basin from the Basque-Cantabrian Basin to the north.

The example of the Berriasian transgression recorded in the W Cameros Basin by establishment of coastal wetland systems matches the interpretations of previous studies in neighboring areas. In those areas, complex coastal systems record transgressions in the innermost parts of the intraplate extensional basins of the Iberian Plate. This observation suggests that this paleogeographic and sedimentological arrangement may be common in the innermost parts of intraplate extensional basins during transgressive episodes throughout the geological record.

KEYWORDS: Coastal wetland, carbonates, Earliest Cretaceous transgression, innermost Iberian Basins, West Cameros sub-Basin, N Spain.

1 INTRODUCTION

Depositional successions developed during the early stages of intraplate extension commonly are dominated by siliciclastic deposits, which pass gradually into carbonate deposits (Gawthorpe and Leeder 2000). These carbonates can be purely continental or show marine influence, depending on their tectonic and paleogeographic setting, as well as on the eustatic context during deposition (Gawthorpe and Leeder 2000). In intra-plate rift systems formed during transgressive episodes marine facies are likely to be deposited in the areas closer to the sea, but the marine influence on the innermost, landward areas of the system can be scarce or hard to detect, and therefore they may have been often overlooked in the geological record. This non-recognition of the marine influence has been frequent in the Tithonian-Berriasian record of the innermost areas of extensional basins of NE Iberian Peninsula.

During the Late Jurassic and Early Cretaceous, two main extensional systems developed in the NE of Iberia: the Basque-Cantabrian Basins Extensional System (BCB) to the N, and the Iberian Basins Extensional System (IB), which crosses the eastern part of the Iberian plate from NW to SE (Fig. 1). A Berriasian transgressive episode has been identified by marine deposits at the distal outermost areas of both IB (e.g. Salas et al. 2001) and BCB (e.g., Pujalte et al. 2004), but the inner landward location of the Cameros Basin within the IB (its innermost NW area, Fig. 1), hindered the deposition of thick marine deposits. Nevertheless, in the eastern sector of the Cameros Basin (Fig, 2A), coastal siliciclastic, carbonate and evaporite deposits, some with tidal influence (Quijada et al. 2013a, 2016a, b), indicate that the Berriasian transgression reached the innermost part of the Iberian Plate and its extensional areas. This study is focused on the western sector of the Cameros Basin (Fig. 2), where Berriasian carbonate sediments have been interpreted as lacustrine in many studies for the last two decades (Platt 1989a,b, 1994, 1995; Clemente and Pérez Arlucea 1993; Mas et al. 1993, 2002, 2003, 2004; Martín Closas and Alonso Millán 1998; Arribas et al. 2003; Schudack and Schudack 2009, 2012; Clemente 2010; Sacristán-Horcajada et al. 2012a,b, 2015, 2016). Nonetheless, some of these studies indicated the presence of foraminifera in the carbonates, suggesting at least local marine influence.

The goal of this study is to analyze the sedimentology of these deposits and to evaluate the extent of marine influence in their sedimentation. Therefore, results will not only help to correlate the W Cameros deposits with coeval units and to reconstruct the paleogeography of NE Iberia during the Berriasian, but they will also contribute to the knowledge of how transgressions can be recorded in the innermost parts of intraplate extensional basins.

2 GEOLOGICAL SETTING

The studied deposits are part of the sedimentary infill of the Cameros Basin, which is located in the northern sector of the Iberian Range (Fig. 2A), and is the northwesternmost basin of the Mesozoic IB (Fig. 1A; Mas et al. 1993; Guimerà et al. 1995; Salas et al. 2001; Mas et al. 2002, 2011). The evolution of Cameros Basin can be divided into four megasequences bounded by main unconformities: the Permian - Triassic Megasequence 1, the Jurassic Megasequence 2, the Latest Jurassic – Early Cretaceous Megasequence 3, and the Late Cretaceous Megasequence 4 (Salas et al. 2001; Mas et al. 2002, 2003, 2011). Two megasequences (1 and 3) correspond to extensional syn-rift phases, and two (2 and 4) correspond to post-extensional, predominantly post-rift thermal, phases (Fig. 1B). In the Cameros Basin, the sedimentary record of Megasequence 3 (Early Tithonian to Early Albian) lies unconformable on top of Middle to Upper Jurassic marine platform deposits of Megasequence 2 (Fig. 2A and B; Fig. 3 A). The sedimentary infill during Megasequence 3 is composed of alluvial, fluvial, lacustrine and coastal sediments (Mas et al. 1993, 2002 and 2011; Sacristán-Horcajada et al. 2012a,b; Quijada et al. 2013a,b, 2016a,b; Suarez-Gonzalez et al. 2013, 2014, 2015, 2016a,b), and is divided into eight depositional sequences (DS) bounded by unconformities (Fig. 3A). During the Alpine Orogeny, the Cameros Basin was inverted, and acquired its current pop-up compressive structure (Fig. 2B). It includes a north-verging, neoformed, main compressional structure that thrusts the Cameros Basin structural unit onto the Cenozoic Ebro Basin, and a south-verging secondary structure that thrusts the Cameros Basin structural unit onto the Duero-Almazán Basin (Fig. 2A and B) (Guimerà et al. 1995; Casas-Sainz et al. 2000).

The Cameros Basin is divided into two sectors (Mas et al., 1993; Fig. 2A): a western sector (W Cameros Basin) and an eastern sector (E Cameros Basin). The E Cameros Basin had the higher subsidence rates, comprising up to 6500 m of sediments (Mas et al. 2002, 2003, 2011; Omodeo-Salé et al. 2014), whereas the W Cameros Basin had much lower subsidence rates, accumulating less than a third of the thicknesses of the eastern sector (Fig. 2B). The current compressive structure of the W Cameros Basin consists of a set of thrusts and folds with a NW-SE orientation (Fig. 2C), limited and cut by strike-slip faults with a NNE-SSW orientation (Beuther 1966; Salomon 1982; Platt 1990; Clemente and Pérez-Arlucea 1993; Guimerà et al. 1995; Martín-Closas and Alonso 1998; Sacristán-Horcajada et al. 2012c, 2015). These structures resulted from inversion of an extensional feature during the Alpine Orogeny, structures that consisted of half-grabens limited by NW-SE normal faults and linked by NNE-SSW transfer zones (Platt 1990; Guimerà et al. 1995; Martín-Closas and Alonso 1998; Sacristán-Horcajada et al. 2012c, 2015). Three different sectors have been distinguished in the W Cameros Basin (Fig. 2C): the northern sector, with southwest-dipping thrusts, which include the area south of the La Demanda Massif; the central sector, which includes the area around the north-dipping Moncalvillo Thrust; and the southern sector, which includes the area around the northeast-dipping San Leonardo Thrust and the South Cameros Thrust.

The focus of this study are deposits representing the third depositional sequence (DS 3) of the Tithonian-Berriasian mega-sequence in the W Cameros Basin (Fig. 3A), which corresponds to the siliciclastic Sandstone and mudstone of the Río del Salcedal Formation and the carbonate Limestone and marl of the Río de San Marcos Formation (hereafter Salcedal Formation and San Marcos Formation, Fig. 3A and B). The relatively poor biostratigraphic data available are based on charophyte and ostracods associations. The charophyte associations indicate that, although the San Marcos Formation contains characteristic flora attributable to the Tithonian - Early Berriasian interval, the Tithonian - Berriasian mega-sequence in its upper part (San Marcos Formation) would reach a Middle Berriasian age (Schudack 1987; Platt 1989b; Martín-Closas and Alonso-Millán 1998). According to Schudack and Schudack (2009, 2012) the ostracod associations indicate that the depositional sequence 2 (DS 2), that is overlain by the depositional sequence under study (DS 3), contains a rich freshwater association consistent with a Berriasian age. Clemente (2010) attributed an Early Berriasian age to the ostracod assemblage in a succession constituted by the Jaramillo, Campolara, Salcedal, and San Marcos Formations (DS 2 and DS 3), which Clemente (2010) considered as a single formation named Rupelo Formation, following the stratigraphic units defined by Platt (1989b). According to all the previous biostratigraphic data, the deposits of this study are considered Early to Middle Berriasian in age.

3 METHODS

General large-scale geological mapping was supplemented by detailed geological mapping of different outcrops at 1:10,000 scale. Twenty-nine stratigraphic sections were studied and sampled in detail (Fig. 2C). A specific sedimentary facies analysis of the third depositional sequence (DS 3) was carried out using enlarged aerial orthophoto scale and outcrop scale field observations and study of more than 100 thin sections. The petrographic analysis included a transmitted-light microscopic examination of polished and uncovered thin sections. The thin sections were prepared using standard procedures including (1) impregnation with blue epoxy resin to highlight porosity and (2) selective staining and etching to identify feldspar (Friedman 1971; Norman 1974) and carbonate minerals (Lindholm and Finkelman 1972).

Regarding the terminology of depositional systems, the term "*coastal wetland*" is used here following geomorphological definitions of modern environments, as applied to ancient deposits by Suarez-Gonzalez et al. (2015). Thus, it refers to a depositional system located in the coastal zone, composed of areas which are partly inundated and partly emerged, due to a fluctuating water table that is at least partially controlled by sea level (Ramsar Convention 2002; Mendelssohn and Batzer 2006; Baldwin et al. 2009; Wolanski et al. 2009).

4 RESULTS

4.1 Stratigraphic architecture of the third depositional sequence (DS3) in W Cameros Basin

The syn-extensional sedimentary record of the W Cameros Basin (Fig. 3B) is divided into seven depositional sequences, which correspond to twelve lithostratigraphic units (Mas et al., 2004). The Tithonian-Berriasian sedimentary record of the W Cameros Basin consists of three depositional sequences (DS 1, DS 2 and DS 3), and includes six formations (Table 1 and Figure 4A-D). DS 3, the focus of this study, appears exclusively in the north sector of the W Cameros Basin (Figs. 4E, F, 5), and comprises two formations. The Salcedal Formation (lower part of DS 3), is 0 to 69 m thick, with a depocenter located in the SE part of the north sector at the Castrovido Section (Figs. 2C, 4E, 5), thinning towards the NW (Fig. 4E). The San Marcos Formation (upper part of DS 3) is 0 to 84 m thick and its depocenter is located in the central-northern part of the north sector at the Rupelo Section (Figs. 2C, 4F, 5). A distinctive feature of the San Marcos Formation is that it contains abundant dinosaur tracks, which are particularly noteworthy at the top of the unit (Torcida Fernández-Baldor et al. 2015). DS 3 also occurs in a small isolated outcrop located in the north-westernmost part of the study area, in which the Arlanzón Section was logged (Fig. 2C). In this section, the Salcedal and San Marcos formations are respectively 34 and 43 m thick.

4.2. Sedimentology of the third depositional sequence (DS 3): Facies Associations

The strata include twelve sedimentary facies: five siliciclastic lithofacies *sensu* Miall (2010) and seven carbonate lithofacies (Table 2). The twelve different sedimentary facies correspond to 9 different types of architectural elements (Figs. 6, 7) *sensu* Miall (2010). In addition, these facies and architectural elements are grouped into 6 distinct facies associations with different environmental significance within the recognized depositional systems (Fig. 7).

4.2.1. Facies Association 1 (FA-1)

FA-1, best represented in the Castrovido section (Fig. 6), is made up of 4 different facies arranged into 5 types of architectural elements (Fig. 7). The most characteristic facies of FA-1 consists on tens of meters-wide lenses of trough cross-bedded sandstone (St). St facies is arranged into sandy bedforms (SB), which are sometimes organized as medium- to large-scale lateral-accretion forms (LA, Fig. 8A) in concave-up erosionally based channel bodies (CH). Paleocurrent data of the cross-bedding are scarce but indicate a predominant W to SW orientation (Fig. 6). The sandy architectural elements are interbedded with floodplain fines (FF), composed mainly of several meters to tens of meters-thick extensive sheets of massive siliciclastic sandy mudstone, which displays root traces and pedogenetic carbonate concretions (Fm). The floodplain fines (FF) contain intercalations of thin sheets of horizontal-bedded and cross-laminated fine sandstone (Sh, Fig. 8A) and paleosol carbonate layers (calcretes) with low lateral continuity and pedogenetic features, such as nodular structure (P).

Interpretation. This association is interpreted as the result of sedimentation of sinuous, channelized bedload in meandering channels and vertical accretion of floodplain deposits in the distal portion of a fluvial system. The concave-up, erosionally based channeled bodies showing medium- to large-scale lateral-accretion forms (SB, CH and LA in Fig. 7), correspond to lateral accretion extensive point-bars on the inside of the channel meander bends (Bridge 2006; Miall 2010). The relatively thick extensive sheets of massive siliciclastic mudstone showing root traces and nodular and massive paleosol carbonate layers stand for vertically accreted floodplain fines in the overbank areas with episodic pedogenetic calcretes formed during drier phases (Bridge 2003 and 2006; Miall 2010; Sacristán-Horcajada et al. 2016). The thin sheets of horizontal-bedded and cross-laminated fine sandstone interbedded with the massive siliciclastic mudstone characterize crevasse splay deposits that directly spread on the floodplain from breaks in the channel bank (Bridge 2006; Miall 2010). The architecture of this facies association shows a net predominance of the suspended load units with respect to the bed load units. This architectural arrangement, together with the lateral accretion recognized in the channeled bodies, indicate a distal fluvial system with a single mobile channel (Friend 1983) that seems to indicate a facies-architecture of the distal zone of a single-thread meandering fluvial system (Davison et al. 2013). It probably corresponds to the distal zone of a relatively small distributive fluvial system (DFS, *sensu* Weissmann et al. 2010, Hartley et al. 2010), likely located northeast of the study area.

4.2.2. Facies Association 2 (FA-2)

FA-2, which occurs only in the uppermost part of the Castrovido section (Fig. 6), is composed of 3 facies and 2 architectural elements (Fig 7). It consists of heterolithic sandy to mixed flat architectural elements (SMF) composed of extensive sheets of rippled wavy- and flaser-bedded sandstone (SrF, Fig. 8B) with some associated channelized trough cross-bedded sandstone that occasionally displays very thin mud laminae between the sandstone foreset laminae (St). These SMF architectural elements are interbedded with extensive sheets of siliciclastic mudstone (Fm) that correspond to mud-flat architectural elements (MF).

Interpretation. This association corresponds to a mixed-flat to mud-flat environment in a siliciclastic tidal flat. The extensive non-channelled heterolithic sheets with wavy- and flaser-bedded sandstone (SrF) interbedded with siliciclastic mudstone (Fm) suggests deposition in broad, flat areas in which episodes of frequent alternating bedload transport and settling from suspension alternated with episodes of exclusive settling from suspension (Klein 1998). Specifically, SrF facies is interpreted as deposited in mid-high intertidal flats due to its similarities with present-day analogues (e.g., Nio and Yang 1991; Dalyrymple 1992, 2010), such as the classical tidal flats of the North Sea (Reineck and Wunderlich 1968; Reineck 1972), and other coastal tidal flats, such as the Baie du Mont Saint Michel (Tessier 1993), San Francisco Bay (Pestrong 1972), the Bay of Fundy (Klein 1985), North West Australia

(Semeniuk 1981), and the Gulf of California (Thompson 1968). A nearly equal period for both suspension and bed load sedimentation occurs in the mid-tidal flats (Klein 1998), generating a tidal rhythmite of interbedded sand and mud (DeRaaf and Boersma 1971; Dalyrymple 2010) similar to that observed in the SrF facies. The associated Fm facies is interpreted to have been deposited in areas in which settling of fine-grained silts and clays predominated, such as present-day high tidal flats. These areas are submerged for less than one third of a tidal cycle, during periods of high water level, when velocities are negligible (Klein 1998). The cross-bedded channeled sandstone with occasional mud-draped foreset laminae (St) would correspond to channel deposits showing tidal bundles, which is also a diagnostic structure associated with sandy bedforms in tidal sedimentary environments (Allen and Homewood 1984; Dalyrymple 2010). These mud-draped cross strata are the result of alternating bedform migration during high flow velocities and mud deposition during high and low tide slackwater in subtidal areas and during exclusively high tide slackwater in intertidal areas.

4.2.3. Facies Association 3 (FA-3)

FA-3 is present in the Rupelo and Arlanzón sections (Fig. 6), and comprises interbedded marls and laterally extensive, centimeter- to meter-thick, carbonate tabular beds (IMC, Figs. 7, 8C). Carbonate beds consist of well-bedded marly foraminiferal limestone and display parallel lamination (Lbf). Locally, disperse rizoliths, black pebbles and desiccation cracks occur on top of Lbf beds (Fig. 8D). The depositional textures are bioclastic mudstone, wackestone and packstone. The biotic association includes benthic foraminifera, such as miliolids and other minute indeterminate forms (Fig. 9A to E), ostracods (Fig. 9B), fish scales and teeth, and gastropods. After ostracods, miliolids (0.5 mm-thick, porcelanous tests) are the most abundant component in the Rupelo section, whereas in the northernmost area (i,e., the Arlanzón section) foraminifera correspond to minute indeterminate forms (trochospiral types, smaller than 0.1 mm. Figs. 9D and 9E). Ostracods have both complete and disarticulated carapaces, their valves are smaller than 0.5 mm, and have a finely prismatic microstructure sometimes with a “cup-in-cup” arrangement (Fig. 9B). Generally, the valves are smooth, but crenulated forms are locally observed. Other minor skeletal grains are charophytes. Micrite matrix is abundant, although it can appear clotted to peloidal and be dolomitized, and it can include mm-scale parallel laminations. Micritic micro-filaments are locally observed. Large (more than 10 mm long) and isolated calcite pseudomorphs after evaporite crystals (gypsum?) are dispersed into a dolomicrite matrix (Fig. 9F). The interbedded marl (Mr) have a massive structure and include the same skeletal grains as Lbf lithofacies (i.e., ostracods, charophytes, and fish scales and teeth).

Interpretation. The low biotic diversity and composition (euryhaline organisms such as benthic foraminifera and ostracods) suggest that this facies association was deposited in restricted, marine-influenced water bodies with rapidly changing salinities. These organisms are adapted to the stressful conditions and are significant producers of carbonate sediments in recent and ancient lagoonal brackish environments (Amstrong and Brasier 2005). Similar biotic associations have been interpreted to develop in ancient coastal lagoonal and peritidal systems (Arribas et al. 1996; López-Martínez et al. 1998, 2006), and in marine-influenced water bodies of ancient coastal wetlands (Suarez-Gonzalez et al. 2015). Clotted to peloidal and filamentous microfabrics suggest microbial-influenced carbonate precipitation. The desiccation cracks and rizoliths, along with black pebbles, are diagnostic of periodical subaerial exposure, suggesting that the shallow marine-influenced water bodies were bordered by palustrine areas. Other early diagenetic processes such as dolomitization and gypsum precipitation are typical components of peritidal environments (Flügel 2010; Warren 2016), and indicate pumping of brackish waters through the original sediment during the last stage of shallowing-upwards elemental sequences. The dolomitization process preserves the depositional texture and is indicative of a very early diagenetic stage.

4.2.4. Facies Association 4 (FA-4)

FA-4 occurs mainly in the Rupelo and Arlanzón sections (Fig. 6), and is composed of massive marl and muddy-silty limestone interbedded with well-bedded marly limestone (IMC, Figs. 7, 8E). Muddy-silty limestones (Lb) are parallel laminated wackestone to packstone with unbroken skeletal grains (Fig. 9G), although some Lb beds are grainstone composed of ostracods, intraclasts and peloids (Fig. 9G, H, I). The biotic association includes mostly ostracods and minor charophytes, fish scales and teeth (Fig. 8F and G), and other undifferentiated skeletal grains. The ostracods, largely of one specie, are abundant, vary in average size (between 0.25 – 0.50 mm), and include both smooth and crenulated valves. Micrite matrix is abundant and is peloidal or locally clotted. Micrite is sometimes dolomitized, preserving a fine crystalline depositional texture. Subaerial exposure features such as desiccation cracks, evaporite pseudomorphs (after probable gypsum crystals), rhizoliths, vuggy porosity, and burrowing by Anelida-like forms is observed on top of Lb limestones.

Interpretation. Ostracodal wackestone and packstone are common in lacustrine sediment of oligotrophic or brackish water lakes (Flügel 2010). Similar facies associations have been described in ancient lacustrine carbonate successions (Arribas 1986; Platt and Wright 1991; Fregenal-Martínez and Meléndez 1994; Bustillo et al. 2002) and water bodies with no marine influence of carbonate coastal wetland areas (Suarez-Gonzalez et al. 2015). The high abundance and low diversity of ostracods (ostracodite microfacies) is typical of lakes and lagoons (Guernet and Lethiers 1989). On the other hand, the variation in the types of ostracod valves (smooth and crenulated) could indicate changes in water salinity, and temperature (Benson et al. 1961; Canudo 2004). Therefore, oligohaline ostracods (smooth valves) can reflect fresh water (very low salinity conditions) whereas euryhaline ostracods (crenulated valves) are characteristic of brackish waters (Canudo 2004). In addition, the presence of evaporite pseudomorphs as well as dolomite can be indicative of a change in the geochemical composition of the interstitial waters in the last stage of the shallowing-upwards sequences (Bustillo et al. 2002), change that could be related to some, occasional, marine influence. This facies association is interpreted as the result of carbonate sedimentation in shallow and quiet water bodies with no to very little marine influence, which underwent periodical salinity changes, as suggested by the presence of pseudomorphfs after Ca-sulphates and early dolomite precipitation (e.g. Warren 2016). Subaerial exposure would produce desiccation cracks and rizoliths. Ichthyologic remains of this and other facies associations can be tentatively assigned to "Ginglymondy indet." (previously *Lepidotes*, Pascual-Arribas et al. 2007), which broadly occur in very different environments: saline, brackish, freshwater, continental and coastal (Bermúdez-Rochas 2015).

4.2.5. Facies Association 5 (FA-5)

This facies association occurs in Campolara and Hortigüela sections, in the upper part of the San Marcos Formation from the central sector of the study area (Fig. 6, Fig. 8H). FA-5 is composed of marls (MTB) and interbedded carbonate tabular beds (CTB) which commonly are arranged in elemental sequences (Fig. 8H). Carbonate beds have either a massive (Lmd) or a nodular structure (Ln) (Fig. 7). Depositional textures are bioclastic wackestone and packstone with dasycladal skeletal grains (Fig. 10A and B). Clotted to peloidal microfabrics are common and micritic filaments are observed only locally. In addition to dasycladales, which are the most common skeletal grain, the fossil association in Lmd includes charophytes (Fig. 10C and D), ostracods (i.e., disarticulated valves smaller than 0.5 mm, either smooth or crenulated), fragments of filamentous calcimicrobial colonies, gastropods and other mollusks. Locally, minute (smaller than 0.1 mm), undetermined benthic foraminifera occur. Desiccation cracks, black pebbles and rhizoliths occur on top of some Lmd beds.

Ln limestones show several features and components that destroy the original components and depositional textures. However, some skeletal grains such as dasycladales, charophytes, ostradods, and mollusks (generally gastropods) are evident. Other features include: nodulization, disperse rhizocretions and rhizoliths (Fig. 10E), circumgranular cracks filled with sparry low magnesium calcite cement, microkarst, breccia, and vuggy porosity partly occluded by geopetal infillings. Carbonate nodules include clotted grains, grumelar peloids and micrite nodules.

Interpretation. The fossil content of this facies association is predominantly dasycladales, charophytes, ostracods and gastropods, which point to sedimentation in coastal carbonate water bodies with probable influence of both fresh- and sea-water, as suggested by the presence of both dasycladales and charophytes. Similar facies associations have been described in ancient, very shallow, brackish coastal lagoons periodically affected by subaerial exposure and pedogenesis in palustrine areas (Arribas 1986; Platt and Wright 1991; Fregenal-Martínez and Menéndez 1994; Alonso-Zarza and Wright 2010), as well as in shallow marine-influenced carbonate water bodies in coastal wetland systems (Suarez-Gonzalez et al. 2015).

4.2.6. Facies Association 6 (FA-6)

FA-6 is the most abundant and representative facies association of the San Marcos Formation (Fig. 6). It is composed of interbedded marls (MTB) and carbonate tabular beds (CTB), including both massive (Lm) and nodular limestone (Ln), which form elemental sequences (Figs. 7, 8H). The massive limestones (Lm) are generally marly and consist of mudstone and wackestone. Clotted to peloidal and filamentous microfabrics are common. The fossil association (Fig. 10F, G) includes charophytes, calcimicrobial filaments, ostracods, and mollusks (generally gastropods). Locally, Lm contains only ostracods (ostracodite facies). Also locally, oncoids and dinosaur tracks are observed (Fig. 8I). Massive limestone (Lm) gradually passes upward to nodular limestone (Ln), which has features, such as nodulization, rhizoliths, black pebbles, circumgranular cracks filled by calcite cement, microkarst, and breccia. Furthermore, carbonate nodules and micronodules, clotted grains and grumelar peloids are very common in Ln. In addition, void (channel) argillaceous cutans and geopetal infilled vug pores related to roots are evident in Ln. Moreover, 0.25-5 mm long, lenticular calcite pseudomorphs after evaporites crystals (probable crystals gypsum) are included in carbonate nodules or dispersed within the micrite matrix (Fig. 10H). All these components and features are similar to those described for Ln lithofacies of the FA-5, which, in fact, is facies change related laterally with FA-6 (Fig. 8H).

Interpretation. The repetitive characteristic sequences of the carbonate tabular beds (massive and nodular limestone) and interbedded marl are similar to those described in fossil shallow carbonate freshwater bodies (Arribas 1986; Platt and Wright 1991; Fregenal-Martínez and Meléndez 1994; Arenas and Pardo 1999; Bustillo et al. 2002; Gierlowsky-Kordesch 2010), which can be associated with coastal environments (Arribas et al. 1996; López-Martínez et al. 1998, 2006; Suarez-Gonzalez et al. 2015). Carbonate sedimentation occurred in shallow freshwater bodies, laterally linked to palustrine areas, and its lateral relationship with FA-5 indicates that sedimentation occurred in water bodies near to other marine-influenced water bodies in a coastal wetland system. The development of pedogenetic elements and features on palustrine limestones (Ln) indicate that these environments were periodically desiccated.

5 DISCUSSION

5.1. General depositional system of the San Marcos Formation

The temporal evolution of the San Marcos Formation records a transgressive trend: starting with non-marine water bodies surrounded by palustrine environments in the earlier stages, and which were progressively replaced by marine-influenced environments (cross-sections A–A’ and B–B’ of Fig. 11). This evolution indicates that during the stages of maximum marine influence, sea-water reached the central part of the studied area, creating a system of shallow and marine-influenced water bodies with carbonate sedimentation (Fig. 11), which received input of fine siliciclastic sediments in its central and southeast part (FA-3 in Fig. 11). This environmental system resulted in the sedimentation of well-bedded, marly, wackestone-packstone limestone and marl with abundant ostracods, benthic foraminifera (dominantly miliolids), scarce charophytes, and fish remains (FA-3). The NW part of this marine-influenced carbonate system had lower siliciclastic input, allowing the development of meadows of dasycladales, recorded in the sedimentation of massive beds of wackestone-mudstone limestone with dasycladales, charophytes, ostracods, scarce benthic foraminifers, gastropods, and bivalves (FA-5). This paleontological association suggests a probable influence of both marine and freshwater, with variable salinity conditions. The shallow marine-influenced water bodies (FA-3 and FA-5) underwent periodic episodes of desiccation and subaerial exposure, as shown by desiccation-cracks in the central and southeastern sector and by pedogenetic calcrete in the northwestern sector. Farther towards the NW (A-A' in Fig. 11), freshwater influence was stronger, as indicated by the higher abundance of charophytes in association with ostracods, gastropods, and bivalves (FA-6). In contrast, towards the SE (A-A' in Fig. 11) marine influence was greater, allowing the development of mixed to muddy siliciclastic tidal flat deposits, consisting of wavy- and flaser-bedded sandstone interbedded with siliciclastic mudstone (FA-2). In turn, this relatively narrow belt of siliciclastic tidal flats connected to the E with the distal portion of a meandering fluvial system (FA-1 in Fig. 7; FA-1 in Fig. 11). This environmental arrangement of restricted marine-influenced water bodies related to a tidal flat is comparable to that interpreted for the lagoon–tidal flat system of the Middle Jurassic Lajas Formation in the Neuquén Basin (McIlroy et al. 2005; Gugliotta et al. 2015).

To the south of the Jaramillo - Covarrubias fault (cross-section B–B' of Figs. 2C and 11), sedimentation was dominated mainly by carbonate deposits, suggesting that it was further away from the input of fine siliciclastic sediments during the stage of maximum marine influence. Towards the SE of this area, carbonates precipitated in shallow, marine-influenced water bodies (FA-5), whereas fresh water bodies and palustrine environments (FA-6) accumulated carbonates towards the NW (Fig. 11). Occasional dinosaur tracks mark the top of the palustrine facies (FA-6).

In the isolated outcrop of the Arlanzón Section (AZ in Figs. 2C, 6A), the San Marcos Formation is dominated by FA-4 and interpreted as a mixed carbonate-fine siliciclastic system with very little to no marine influence (Fig. 6A). This area was a small sub-basin and had input of fine siliciclastic sediments from a fluvial system, probably from the south as explained below. Marine influence in this sub-basin is shown by sedimentation of well-bedded wackestone-packstone marly limestone to marl, with abundant ostracods, and scarce charophytes and benthic foraminifera (FA-3 in Fig. 7), as well as by the precipitation of early dolomite and Ca-sulphates. Short desiccation stages affected this area, as evidenced by the presence of desiccation-cracks and gypsum pseudomorphs.

The different facies associations recorded throughout the Berriasian DS3 deposits of W Cameros Basin (Fig. 11) define a complex depositional system composed of many interrelated carbonate and mixed carbonate-siliciclastic environments with contrasting conditions that range from freshwater to tide-influenced, all surrounded by palustrine areas and located in the continental-marine transition. This complex interrelation of contrasting environments is analogous to that observed in modern wide and flat coastal areas, which are prone to rapid spatial and temporal variations, being easily flooded but also easily desiccated (e.g. Lacovara et al. 2003; Wilkinson and Drummond 2004; Maloof and Grotzinger 2012). The most suitable and widely-used general terminological classification for modern coastal systems with both continental and marine signatures is 'coastal wetlands' (cf. Ramsar Convention 2002; Mendelssohn and Batzer 2006; Baldwin et al. 2009; Wolanski et al. 2009). This term was not commonly used for ancient depositional systems (only sporadically and unsystematically for some fossil coal-bearing transitional units: Greb and DiMichele 2006) until Suarez-Gonzalez et al. (2013, 2015) applied it to the detailed paleoenvironmental classification of complex Lower Cretaceous deposits, similar to those described here, in the neighboring E Cameros Basin. Since then, other ancient deposits, from many different ages and localities, have been observed to match the sedimentological features and criteria proposed by Suarez-Gonzalez et al. (2015) for ancient coastal wetland depositional systems (Marmi et al. 2014; Costamagna 2016; Di Celma et al. 2016; Fondevilla et al. 2017; Millward et al. 2018). Therefore, given the similarities of all these complex transitional deposits with the Berriasian deposits of the W Cameros Basin described here, it is interpreted that the most appropriate classification for this complex system as a whole is a carbonate coastal wetland.

5.2. General paleogeographic setting of the Berriasian transgresion in the W Cameros Basin

The sedimentary record of the San Marcos Formation is documented only in the northern sector of the W Cameros Basin, specifically to the NW of the Jaramillo-Covarrubias Fault and in the isolated small basin of Arlanzón (AZ), located to the north (Figs. 4F, 12). The depositional system recorded in this unit had two different sedimentary distributions, interpreted to be deposited during a general transgression: early long periods characterized by development of carbonate-producing water bodies with no to little marine influence and palustrine environments (Fig. 13A), followed by shorter periods of marine-influenced water bodies characterized by carbonate and mixed carbonate-siliciclastic sedimentation (Fig. 13B).

During the stage of maximum marine influence (Fig. 13B), a coastal wetland system developed in the N sector and Arlanzón area (framed area in Fig. 12). The water bodies occupied the central part of the North Sector (FA-3) and received fine siliciclastic input from the east, associated with a siliciclastic intertidal flat rim (FA-2) and with the distal zone of a distributive fluvial system (FA-1). Shallow, marine-influenced carbonate (FA-5) developed laterally in the areas with minor terrigenous input. The spatial arrangement of the different environments of this coastal system indicates that marine influence may have reached the studied area directly from the north (Figs. 13B, 14), that is, from the BCB (Fig. 1), as previously suggested (Platt and Pujalte 1994). Thus, this arrangement would imply that during the Berriasian, the BCB was interconnected with the northwesternmost sector of the IB (Cm in Fig. 1, WC in Fig. 14), probably by an intermediate system of relatively small basins controlled by extensional tectonics (e.g., Polientes, Sedano, and Rioja Trough Sub-Basins; Klimowitz et al. 1999, 2005; Cámara 1997, 2014; Mas et al. 2002, 2003, 2004). In fact, Benito et al. (2005) noted that, previously, during the Late Kimmeridgian, marine influence reached the Cameros area from the north, and not from the south as it was traditionally considered (Mas et al. 2004 and references therein). These researchers concluded that the northern Boreal realm was nearer to the Cameros area than the southeastern Tethyan realm, and this proximity probably persisted throughout the Upper Jurassic and Early Cretaceous (Quijada et al. 2013a, 2016a, b; Suarez-Gonzalez et al. 2013, 2015, 2016b).

The interpretation of a Berriasian paleogeographic connection between the W Cameros Basin and the BCB, to the north (Fig. 1), motivates a reconsideration of the general paleogeographic setting of the NE Iberian Peninsula during this period. In previous decades, the interpretation that the northwestern Cameros area belongs to the large-scale tectonic unit of the IB (Fig. 1, Mas et al. 1993; Guimerà et al. 1995; Salas et al. 2001), led Mas et al. (1993, 2002) to suggest that the different marine incursions recorded in the Cameros Basin (during Tithonian-Berriasian and Upper Barremian-Aptian times), reached this basin from the SE (i.e. the Tethyan realm, along the IB). In the case of the Berriasian period, this interpretation was maintained in later works (Mas et al. 2004, 2011), until Quijada et al. (2013a, 2016a, b) presented new data from the E Cameros Basin, which indicated a northern marine link between that basin and the BCB. Nevertheless, these authors did not totally discard the possibility of a marine influence from the SE, through a tentative correlation with the deposits of the Villar del Arzobispo Formation (South-Iberian Basin, Fig. 1), which traditionally were considered Upper Tithonian-Middle Berriasian in age (Aurell et al. 1994; Mas et al. 2004). However, recent studies of the Villar del Arzobispo Formation have brought to light new micropaleontological and stratigraphic data that reassess its age as Kimmeridgian-Tithonian (Campos-Soto et al. 2016, 2017), thus impeding the correlation between this unit and the Berriasian DS 3 deposits of both E and W Cameros Basin.

Taking all these data into account, the new interpretation of the W Cameros Berriasian deposits presented here seems to be more consistent with an interpretation of a paleogeographic connection between the Berriasian Cameros Basin and the BCB, rather than with the IB (Fig. 14). The Berriasian BCB shows a transition from continental and coastal deposits in W and SW areas towards clear marine deposits in E and NE areas (Fig. 14; García de Cortázar and Pujalte 1982; Pujalte 1982; Lanaja and Navarro 1987; Pujalte et al. 2004, and references therein). Therefore, during the stage of maximum marine influence in the deposits studied here, both the Berriasian transgression and the syn-sedimentary tectonics (see next section) may have produced the entrance of seawater into the W Cameros Basin, connecting it to the BCB, in which the Berriasian Aroco and Loma Somera Formations were being deposited (Pujalte 1982; García de Cortázar and Pujalte 1982; Pujalte et al. 2004). Furthermore, the Berriasian deposits of the E Cameros have also been interpreted as paleogeographically connected with coeval BCB deposits (Quijada et al. 2013a, 2016a,b), but there are no preserved outcrops of Berriasian deposits in the linkage zone between them (Fig. 14; Quijada et al. 2013a). Nevertheless, the new results of the W Cameros Basin presented here suggest that perhaps during the stage of maximum marine influence both sub-basins could have been linked paleogeographically as suggested by the siliciclastic tidal flats of the Berriasian Salcedal Formation (W Cameros). These deposits bordered the eastern side of the marine-influenced deposits (FA-2 in Fig. 13B), and may have bordered the distal fluvial system towards the east (FA-1 in Fig. 13B), eventually connecting with the siliciclastic tidal flats of the Berriasian Huérteles Formation (Oncala Group) of the E Cameros Basin (Fig. 14; Quijada et al. 2016a).

5.3. Factors controlling the sedimentation and paleogeography in W Cameros Basin: An example for interpreting transgressive episodes in the innermost areas of extensional basins.

The main allogenic controls on deposition in intraplate extensional systems are: tectonics, eustasy and climate. Concerning the sedimentation of the W Cameros Basin Berriasian deposits described here, synsedimentary tectonics was a very important factor, because in this area different tectonic structures controlled the thickness and distribution of these deposits. NW-SE normal faults with associated NE-SW transfer zones compartmentalized the N sector of W Cameros Basin in several NW-SE elongated areas with different subsidence rates (framed area in Fig. 12), reflected in different deposit thicknesses. The depocenter (Fig. 4E and F) was located just to the NW of the NE-SW Jaramillo-Covarrubias Transfer Zone (Fig. 12). The thickness of the studied deposits decreases towards the S of the

Quintanilla-Hortigüela Fault and towards the N of the Palazuelos de la Sierra Fault (Fig. 12). The deposits of the San Marcos Formation did not surpass the Jaramillo-Covarrubias Transfer Zone (Fig. 4, and 4 in Fig. 12), indicating that this NE-SW transfer zone also played an important role in its sedimentation. Moreover, several observations are consistent with an interpretation that the fault systems also controlled the distribution of sedimentary environments. In the N sector, carbonate and mixed depositional environments were bounded by the NE-SW Jaramillo - Covarrubias Transfer Zone. To the SE of this transfer zone, fluvial meandering siliciclastic environments were predominant (Fig. 4; FA-1 in Figs. 13A, B). The shallow, carbonate, water bodies with little to no marine influence and fine siliciclastic input from the E occupied an area near the Jaramillo-Covarrubias Transfer Zone, but did not extend towards the SW beyond the Quintanilla-Hortigüela Fault (FA-4 in Fig. 13A). During the period of maximum marine influence, shallow, marine-influenced carbonates with fine siliciclastic input from the E also occupied an area near the Jaramillo-Covarrubias Transfer Zone, without surpassing the Quintanilla-Hortigüela Fault (FA-3 in Fig. 13B). Distal fluvial meandering streams and a siliciclastic tidal flat occupied the SE area (FA-1 and FA-2 in Fig. 13B). Finally, in the northern Arlanzón sector, the Riocavado de la Sierra Fault (Fig. 2C, 3 in Fig. 12), which crosses the SW of La Demanda Massif (Fig. 2C) and is probably the SE continuation of the Late Variscan Ventaniella Fault of the Cantabrian Mountains (Vegas and Banda 1982; Capote et al. 2002; Suarez-Gonzalez et al. 2016b), seems to have controlled the evolution of the small Arlanzón basin (AZ in Figs. 13A, B), allowing the development of carbonate coastal wetlands during the sedimentation of the San Marcos Formation.

In the W Cameros Basin all these NW-SE and NE-SW tectonic structures have traditionally been interpreted as the product of the reactivation of previous Late Variscan strike-slip faults as normal faults (the NW-SE structures) and transverse faults (the NE-SW structures) during the Late Jurassic – Early Cretaceous extensional phases (Platt 1990, 1995; Arribas et al. 2003; Sacristán-Horcajada et al. 2015). Subsequently, during Alpine contraction, the NW-SE normal faults became thrusts and reverse faults and the NE-SW transverse faults became strike-slip faults (Platt 1990, Guimerà et al. 1995, 2004; Sacristán-Horcajada et al. 2015). Similarly, the role of reactivated Late Variscan faults has also been shown to be relevant in the sedimentation of Early Cretaceous syn-extensional deposits of the neighboring E Cameros Basin (Suarez-Gonzalez et al. 2016b). The stratigraphic and sedimentological data presented here further support the previous interpretations about the important role of the extensional reactivation of Late Variscan tectonic structures during the sedimentation of the Berriasian W Cameros deposits. In fact, the role of those structures in the generation of sedimentary basins, at the scale of the whole Iberian Plate, has been recently emphasized in new models of the tectonic evolution of the whole Iberian-European Plate Boundary, both in the Boreal and Tethyan domain, during the Late Jurassic – Early Cretaceous extensional phases (Tugend et al. 2014, 2015; Fig. 15).

Therefore, the strong fault control on the facies distribution and thickness of the studied deposits highlights that tectonics was a crucial allogenic factor. Nevertheless, the marine influence in the sedimentation of these deposits also suggests that eustatic variations were a further control in their sedimentation. The stages of marine influence in the San Marcos Formation probably corresponded to the upper Early Berriasian (*Subthurmannia occitanica* zone) sea level rise and consequent transgressive cycle that occurred in both Boreal and Tethyan European basins ("Middle Berriasian" *sensu* Hardenbol et al. 1998 who differentiated Early, Middle, and Late Berriasian; and "upper Early Berriasian" *sensu* Ogg et al. 2008, 2012 who exclusively differentiated Early, and Late Berriasian). Thus, during the stage of maximum marine influence in the W Cameros Basin, the gains of accommodation linked to a eustatic rise added to that due to gains of tectonic subsidence, increased the total accommodation, and favored marine transgression and the development of a carbonate coastal wetland system (Fig. 13B).

The last factor that may have influenced the sedimentation of the studied deposits is climate. The coastal wetlands of the San Marcos Formation underwent periodically long episodes of desiccation and subaerial exposure, suggesting a semiarid seasonal setting. Moreover, in the neighboring E Cameros Basin, the coeval Berriasian Oncala Group includes tide-influenced fluvial deposits laterally related with thick evaporite deposits, which were partially deposited in extensive, shallow, carbonate-sulphate coastal salinas that received seawater input mostly from the north (Quijada et al. 2013a, b, 2014, 2016a,b). In addition, just north of the W Cameros Basin, in the southernmost part of the BCB, Diéguez et al. (2009) described fossils of xerophytic macroflora in the Aguilar Formation (Upper Tithonian-Lower Berriasian, Pujalte et al. 2004), probably developed in dry-savannah environments. All these observations support the interpretation that the San Marcos Formation coastal wetlands were deposited under a semiarid to arid climate that caused the seasonal alternation of short wet and long dry periods. This interpretation matches the global geological record, which indicates widespread arid conditions across much of Europe at the beginning of the Upper Jurassic, as well as in southern Eurasia during the Upper Jurassic-Early Cretaceous (Hallam 1984, 1985; Hallam et al. 1993; Vakhrameev 1991; Ziegler et al. 1993).

In summary, during the Berriasian transgressive episode, the combination of tectonics and eustasy, together with climatic factors, led to the establishment of a complex mixed carbonate-siliciclastic coastal wetland system in the W Cameros Basin, which was located at the innermost area of an intraplate extensional system. In the neighboring E Cameros Basin, the Berriasian transgressive episode (Quijada et al. 2013a,b, 2014, 2016a,b), as well as other Early Cretaceous transgressions (Suarez-Gonzalez et al. 2013, 2015), caused the development of complex and wide coastal depositional systems, all of them linked to the influence of marine water coming from the northern BCB. Therefore, the paleogeographic arrangement that allows the development of those complex coastal systems at the innermost part of intraplate extensional basins may be common to many other extensional systems throughout the geological record, and thus, the Cameros Basin may be proposed as a model for the record of transgressive events in the internal areas of those systems, in which the combination of tectonics, eustasy and climate are very likely to produce wide mixed carbonate-siliciclastic-evaporitic coastal systems with a complex mixture of continental and shallow-marine features.

6 CONCLUSIONS

A marine transgression reached the W Cameros Basin during the sedimentation of its Early-Middle Berriasian third depositional sequence (DS 3), which consists of siliciclastic deposits (Salcedal Formation) that gradually change laterally and vertically to carbonate and mixed carbonate-siliciclastic deposits (San Marcos Formation).These units are interpreted as deposited in a complex mixture of carbonate and –siliciclastic environments located in the continental-marine transition, which is interpreted here as a coastal wetland system. A semiarid to arid climate characterized by the seasonal alternation of short wet and long dry periods predominated, causing water bodies of the system to undergo periodic desiccation and subaerial exposure.

The spatial distribution of paleoenvironments indicates that marine influence reached the W Cameros Basin from the Basque-Cantabrian Basin, located to the north. During the maximum marine influence stage (probably the Middle Berriasian global sea level rise), the gains of accommodation linked to a Berriasian eustatic rise was added to the gains of accommodation due to tectonic subsidence, favoring the marine incursion in the W Cameros Basin. This Early-Middle Berriasian marine influence in the

Cameros Basin exclusively from the north prompts a reevaluation of the general paleogeography of NE Iberian Peninsula for the Berriasian.

The establishment of wide and complex coastal wetland systems during the peak of a transgressive episode in the W Cameros Basin, matches the interpretations of previous studies in neighbouring areas, where also multifaceted coastal systems where recorded during transgressions in the innermost parts of the intraplate extensional basins of the Iberian Plate. Therefore, the development of such complex depositional systems, with both continental and marine signatures, is suggested here to be a result of the interplay between tectonics and eustasy that may be characteristic of internal extensional basins during transgressive periods.

7 ACKNOWLEDGMENTS

The authors are grateful to Dr. Ramon Salas and an anonymous referee for their thorough revision of the manuscript. We want to extend our thanks to Dr. Edoardo Perri, Dr. Brian Pratt, and Dr. Gene Rankey as their detailed comments and suggestions have helped us to significantly improve our work. Funding for this research was provided by the Spanish Ministry of Economy and Competitivity, projects CGL2011-22709 and CGL2014-52670-P, and by the research group ‘‘Sedimentary Basin Analysis’’ UCM 910429 of the Complutense University of Madrid, and by the Geosciences Institute (IGEO-CSIC). We thank also the Departments of Geodynamics, Stratigraphy, and Paleontology and Mineralogy and Petrology of the Complutense University of Madrid and the IGEO (CSIC) for their technical support.

REFERENCES

Allen, P.A., & Homewood, P. (1984). Evolution and mechanics of a Miocene tidal sandwave. *Sedimentology*, 31, 63–81.

Alonso-Zarza, A.M., & Wright, V.P. (2010). Calcretes. In A.M. Alonso-Zarza, and L.H. Tanner (Eds.), *Carbonates in Continental Settings: Facies, Environments and Processes* (pp. 225–267). Amsterdam: Elsevier.

Arenas, C., & Pardo, G. (1999). Latest Oligocene – Late Miocene lacustrine systems of the north-central part of the Ebro Basin (Spain): sedimentary facies model and palaeogeographic synthesis. *Palaeogeography, Palaeoclimatology and Palaeoecology*, 151, 127-148.

Armstrong, H.A., & Brasier, M. D. (2005). *Microfossils*. Malden, Blackwell Publishing, 304 p.

Arribas, J., Alonso, A., Mas, R., Tortosa, A., Rodas, M., Barrenechea, J.F., Alonso-Azcárate, J., & Artigas, R. (2003). Sandstone petrography of continental depositional sequences of an intraplate rift basin: Western Cameros Basin (North Spain). *Journal of Sedimentary Research*, 73, 309-327.

Arribas, M.E. (1986). Petrología y análisis secuencial de los carbonatos lacustres del Paleógeno del sector N de la Cuenca Terciaria del Tajo. *Cuadernos de Geología Ibérica*, 10, 295–334.

Arribas, M.E., Ardèvol, Ll. & López-Martínez, N. (1996). Lacustrine peritidal carbonates in the Upper cretaceous Tremp Formation (Àger syncline, Pyrenean foreland Basin, Spain). In *17th Regional African European meeting of Sedimentology*, Abstracts, p.15.

Arthaud, F., & Matte, P. (1977). Late Paleozoic strike-slip faulting in southern Europe and northern Africa: result of a right-lateral shear zone between the Appalachians and the Urals. *Bulletin of the Geological Association of America*, 88, 1305-1320.

Aurell, M., Mas, R., Meléndez, A., & Salas, R. (1994). El tránsito Jurásico - Cretácico en la Cordillera Ibérica: relación tectónica-sedimentación y evolución paleogeográfica: *Cuadernos de Geología Ibérica*, 18, 369-396.

Baldwin, A.H., Barendregt, A., & Whigham, D. (2009). Tidal freshwater wetlands: an introduction to the ecosystem. In A. Barendregt, D. Whigham, and A. Baldwin (Eds.), *Tidal Freshwater Wetlands* (pp. 1–10). Leiden: Backhuys.

Benito, M.I., Lohmann, K.C., & Mas, R. (2005). Paleogeography and paleoclimate in the Northern Iberian Basin of Spain: constraints from diagenetic records in reefal and continental carbonates. *Journal of Sedimentary Research*, 75, 82-96.

Benson, R. H., Berdan J. M., Van den Bold, W. A., Hanai, T., Hessland, l., Howe, H.V., et al., (1961). Part Q, Arthropoda: Crustacea: Ostracoda. In R. C. Moore (Ed.), *Treatise on*

Invertebrate Paleontology (pp. 1-432). Kansas: Geologica1 Society of America and University of Kansas Press.

Bermúdez-Rochas, D.D. (2015). *Ictiofaunas del Cretácico inferior de las cuencas Vasco-Cantábrica y de Cameros en el registro español del Mesozoico - Early Cretaceous Ichthyofaunas from the Basque-Cantabrian and Cameros basins in the Spanish Mesozoic record.* Unpublished Ph.D. Thesis. Universidad Complutense de Madrid. Spain. 593 pp.

Beuther, A. (1966). Geologische Untersuchungen in Wealden und Utrillas-Schichten im Westteil der Sierra de los Cameros (Nordwestliche Iberische Ketten). *Beihefte zum Geologischen Jahrbuch*, 44, 103-121.

Bridge, J. S. (2003). *Rivers and Floodplains: Forms, Processes and Sedimentary Record*. Oxford, Blackwell, 491 p.

Bridge, J. S. (2006). Fluvial facies models: recent developments. In H. W. Posamentier and R. G. Walker (Eds.), *Facies Models Revisited* (pp. 85-170). Tulsa: SEPM Special Publication 84.

Bustillo, A., Arribas, M.E. & Bustillo, M. (2002). Dolomitization and silicification in low-energy lacustrine carbonates (Paleogene, Madrid Basin, Spain). *Sedimentary Geology*, 151, 107-126.

Cámara, P. (1997). The Basque-Cantabrian basin's Mesozoic tectono-sedimentary evolution. *Mémoires de la Société Géologique de France*, 171, 187-191.

Cámara, P. (2014). *Excursión de Campo. Cuenca Vasco-Cantábrica, Transversal Ayoluengo-Bilbao-Bermeo*. Asociación de Geólogos y Geofísicos Españoles del Petróleo, pp. 120.

Campos-Soto, S., Benito, M. I., Mas, R., Caus, E., Cobos, A., Suarez-Gonzalez, P., & Quijada, I.E. (2016). Revisiting the Late Jurassic-Early Cretaceous of the NW South Iberian Basin: new ages and sedimentary environments. *Journal of Iberian Geology*, 42, 69-94.

Campos-Soto, S., Cobos, A., Caus, E., Benito, M.I., Fernandez-Labrador, L., Suarez-Gonzalez, P., Quijada. I.E., Mas, R., Royo-Torres, R., & Alcalá, L. (2017). Jurassic Coastal Park: A great diversity of palaeoenvironments for the dinosaurs of the Villar del Arzobispo Formation (Teruel, E Spain). *Palaeogeography, Palaeoclimatology, Palaeoecology*, 485, 154-177.

Canudo, J. I. (2004). Ostrácodos. In E. Molina (Ed.), *Micropaleontología* (pp. 441 – 460). Zaragoza: Prensas Universitarias de Zaragoza.

Capote, R., Muñoz, J. A., Simón, J. L., Liesa, C. L., & Arlegui, L. E. (2002). Alpine tectonics I: the Alpine system north of the Betic Cordillera. In W. Gibbons and M. T. Moreno (Eds.), *The geology of Spain* (pp. 367–400). London: Geological Society of London, Special Publication.

Casas-Sainz, A. M., Cortés-Gracia, Á. L., & Maestro-González, A. (2000). Intraplate deformation and basin formation during the Tertiary within the northern Iberian plate: origin and evolution of the Almazán Basin. *Tectonics*, 19, 258-289.

Clemente, P. (2010). Review of the Upper Jurassic-Lower Cretaceous stratigraphy in Western Cameros Basin, Northern Spain. *Revista de la Sociedad Geológica de España*, 23 (3-4), 101-143.

Clemente, P., & Pérez-Arlucea, M. (1993). Depositional architecture of the Cuerda del Pozo Formation, Lower Cretaceous of the extensional Cameros Basin, north-central Spain. *Journal of Sedimentary Petrology*, 63, 437-452.

Costamagna, L.G. (2016) The Middle Jurassic Alpine Tethyan unconformity and the Eastern Sardinia – Corsica Jurassic high: A sedimentary and regional analysis. *Journal of Iberian Geology*, 42, 311-334.

Dalrymple, R.W. (1992). Tidal depositional systems. In R.G. Walker and N.P. James (Eds.), *Facies Models: Response to sea level changes* (pp. 195–218). St. John's, Newfoundland: Geological Association of Canada.

Dalrymple, R.W. (2010). Tidal depositional systems. In N.P. James and R.W. Dalrymple (Eds.), *Facies Models* (pp. 201-231). St. John's, Newfoundland: Geological Association of Canada.

Davidson, SK., Hartley, A.J., Weissmann, G.S., Nichols, G.J., & Scuderi, L.A. (2013). Geomorphic elements on modern distributive fluvial systems. *Geomorphology*, 180–181, 82–95.

DeRaaf, J.F.M., & Boersma, J.R. (1971). Tidal deposits and their sedimentary structures. *Geologie en Mijnbouw*, 50, 479-504.

Di Celma, C., Fagaini, L., Caffau, M. (2016) Marine and nonmarine deposition in a long-term low-accommodation setting : An example from the middle Pleistocene Qm2 unit, eastern central Italy. *Marine and Petroleum Geology*, 72, 234-253.

Diéguez, C., Hernández, J.M., & Pujalte, V. (2009). A fern-bennettitalean floral assemblage in Tithonian - Berriasian travertine deposits (Aguilar Formation, Burgos - Palencia, N Spain) and its palaeoclimatic and vegetational implications. *Journal of Iberian Geology*, 35 (2), 127-140.

Flügel, E. (2010). *Microfacies of Carbonate Rocks: Analysis, Interpretation and Application*. Heidelberg: Springer, 984 p.

Fregenal-Martínez, M.A., & Meléndez, N. (1994). Sedimentological analysis of the Lower Cretaceous lithographic limestones of the ‘‘Las Hoyas’’ fossil site (Serranía de Cuenca, Iberian Range, Spain). *Geobios*, 16, 185–193.

Friedman, G.M. (1971). Staining. In R.E. Arver (Ed.), *Procedures in Sedimentary Petrology* (pp. 511–530). New York: Wiley.

Friend, P. (1983). Towards the field classification of alluvial architecture or sequence. In J.D. Collinson and J. Lewint (Eds.), *Modern and ancient fluvial systems* (pp. 195-206). Oxford: Blackwell Science, International Association of Sedimentologists, Special Publication 6.

Fondevilla, V., Vicente, A., Battista, F., Sellés, A.G., Dinarès-Turell, J., Martín-Closas, C., Anadón, P., Vila, B., Razzolini, N.L., Galobart, À., Oms, O. (2017) Geology and taphonomy of the L’Espinau dinosaur bonebed, a singular lagoonal site from the Maastrichtian of South-Central Pyrenees. *Sedimentary Geology*, 355, 75-92.

García de Cortázar, A., & Pujalte, V. (1982). Litoestratigrafía y facies del Grupo Cabuérniga (Malm-Valanginiense inferior?) al S de Cantabria-NE de Palencia. *Cuadernos de Geología Ibérica*, 8, 5-21.

Gawthorpe, R.L., & Leeder, M.R. (2000). Tectono-sedimentary evolution of active extensional basins. *Basin Research*, 12, 195-218.

Gierlowsky-Kordesch, E. H. (2010). Lacustrine carbonates. In A. M. Alonso-Zarza and L. Tanner (Eds.), *Carbonates in Continental Settings* (pp. 2-50). Amsterdam: Elsevier. Developments in Sedimentology, 61.

Guernet, C., & Lethiers, F. (1989). Ostracodes et recherche des milieux anciens: possibilities and limites. *Bulletin de la Société géologique de France*, 8, 577-588.

Gugliotta, M., Flint, S. S., Hodgson, D. M., & Veiga, G. D. (2015). Stratigraphic record of river-dominated crevasse subdeltas with tidal influence (Lajas Formation, Argentina). *Journal Sedimentary Research*, 85, 265–284.

Guimerà, J., Alonso, Á., & Mas, J. R. (1995). Inversion of an extensional-ramp basin by a newly formed thrust: the Cameros Basin (N. Spain). In J. G. Buchanan and P. G. Buchanan (Eds.), *Basin Inversion* (pp. 433-453). London: Geological Society, Special Publications, 88.

Guimerà, J., Mas, R., & Alonso, Á. (2004). Intraplate deformation in the NW Iberian Chain: Mesozoic extension and Tertiary contractional inversion. *Journal of the Geological Society*, 161, 291-303.

Hallam, A. (1984). Continental humid and arid zones during the Jurassic and Cretaceous. *Palaeogeography, Palaeoclimatology, Palaeoecology*, 47, 195-223.

Hallam, A. (1985). A review of Mesozoic climates. *Journal of the Geological Society*, 142, 433-445.

Hallam, A., Crame, J. A., Mancenido, M. O., Francis, J., & Parrish, J. T. (1993). Jurassic climates as inferred from the sedimentary and fossil record. *Philosophical Transactions of the Royal Society of London*, B, 341, 287-296.

Hardenbol, J., Thierry, J., Farley, M.B., Jacquin, Th., de Graciansky, P. C., Vail, P.R., et al. (1998). Mesozoic and Cenozoic sequence chronostratigraphic framework of European basins. In P. C. de Graciansky, J., Hardenbol, Th., Jacquin, & P.R., Vail, (Eds.), *Mesozoic-Cenozoic Sequence Stratigraphy of European Basins* (pp. 3e13, 763e781, and chart supplements). Tulsa: SEPM Special Publication, 60.

Hartley, A.J., Weissmann, G.S., Nichols, G.J., & Warwick, G.L. (2010). Large distributive fluvial systems: Characteristics, distribution, and controls on development. *Journal of Sedimentary Research*, 80, 167-183.

Klein, G. de V. (1985). Intertidal flats and intertidal sand bodies. In R. A. Jr. Davis, (Ed.), *Coastal sedimentary environments* (pp. 187-224). New York: Springer-Verlag.

Klein, G.D. (1998). Clastic Tidalites - a partial retrospective view. In C. R. Alexander, R. A. Davis, & V. J. Henry, (Eds.), *Tidalites Processes and Products* (pp. 5-14). Tulsa: SEPM, Special Publication, 61.

Klimowitz, J., Malagón, J., Quesada, S., & Serrano, A. (1999). Desarrollo y evolución de estructuras salinas mesozoicas en la parte suroccidental de la Cuenca Vasco-Cantábrica (norte de España): implicaciones exploratorias. In AGGEP (Ed.), *Libro homenaje a José Ramírez del Pozo* (pp. 159-166). Madrid: Asociación de Geólogos y Geofísicos Españoles del Petróleo.

Klimowitz, J., Ruíz, G., Hernandez, E., & Pérez, A. (2005). Caracterización estratigráfica de la serie Purbeck en el área de Polientes-Sedano y las franjas plegadas de Montorio y Zamanzas (Cuenca Cantábrica). In AGGEP (Ed.), *Aniversario AGGEP* (Libro XXV, pp. 163-168). Madrid: Asociación de Geólogos y Geofísicos Españoles del Petróleo.

Lacovara, K.J., Smith, J.R., Smith, J.B., & Lamanna, M.C. (2003) The Ten Thousand Islands coast of Florida: a modern analog to low-energy mangrove coasts of Cretaceous epeiric seas. In Davis, R.A., Sallenger, A., and Howd, P. (Eds.), *Proceedings of the 5th International conference on Coastal Sediments: New Jersey*, World Scientific Publishing, p. 1773–1784.

Lanaja, J.M., & Navarro, A. (1987). *Contribución de la exploración petrolífera al conocimiento de la Geología de España*. Madrid: I.G.M.E., 465 p.

Lindholm, R.C., & Finkelman, R.B. (1972). Calcite staining: semiquantitative determination of ferrous iron. *Journal of Sedimentary Petrology*, 42, 239–242.

López-Martínez, N., Ardevol, L., Arribas, M.E., Civis, J., & González-Delgado, A. (1998). The Geological record in non-marine environments around the K/T boundary (Tremp Fm, Spain). *Bulletin de la Socièté géologique de France*, 169 (1), 11-20.

López-Martínez, N., Arribas, M.E., Robador, A., Vicens, E., & Ardèvol, Ll. (2006). Los carbonatos danienses (Unidad 3) de la Formación Tremp (pirineos sur-centrales): paleogeografía y relación con el límite Cretácico-Terciario. *Revista de la Sociedad Geológica de España*, 19 (3-4), 233-255.

Maloof, A.C. & Grotzinger, J.P. (2012) The Holocene shallowing-upward parasequence of north-west Andros Island, Bahamas. *Sedimentology*, 59, 1357–1407.

Marmi, J., Vila, B., Martín-Closas, C., Villalba-Breva, S. (2014) Reconstructing the foraging environment of the latest titanosaurs (Fumanya dinosaur tracksite, Catalonia). *Palaeogeography, Palaeoclimatology, Palaeoecology* 410, 380-389.

Martín-Closas, C., & Alonso, A. (1998). Estratigrafía y biostratigrafía (Charophyta) del Cretácico inferior en el sector occidental de la Cuenca de los Cameros (Cordillera Ibérica). *Revista de la Sociedad Geológica de España*, 11, 253-270.

Mas, R., Alonso, A., & Guimerà, J. (1993). Evolución tectonosedimentaria de una cuenca extentional intraplaca: La cuenca finijurásica-eocretácica de Los Cameros (La Rioja-Soria). *Revista de la Sociedad Geológica de España*, 6, 129–144.

Mas, R., Benito, M.I., Arribas, J., Serrano, A., Guimerà, J., Alonso, A., & Alonso-Azcarate, J. (2002). La Cuenca de Cameros: desde la extensión finijurásica-eocretácica a la inversión terciaria – implicaciones en la exploración de hidrocarburos. *Zubía*, 14, 9-64.

Mas, J.R., Benito, M.I., Arribas, J., Serrano, A., Alonso, A., & Alonso-Azcárate, J. (2003). The Cameros Basin: From Late Jurassic-Early Cretaceous Extension to Tertiary Contractional Inversion-Implications of Hydrocarbon Exploration. In AAPG ((Ed.), *Geological Field Trip 11* (pp.56). Barcelona: AAPG International Conference and Exhibition.

Mas, R., García, A., Salas, R., Meléndez, A., Alonso, A., Aurell, M., Bádenas, B., Benito, M.I., Carenas, B., García-Hidalgo, J.F., Gil, J., & Segura, M. (2004). Segunda fase de rifting: Jurásico Superior-Cretácico Inferior. In J.A. Vera, (Ed.), *Geología de España* (pp. 503-510). Madrid: SGE-IGME.

Mas, R., Benito, M.I., Arribas, J., Alonso, A., Arribas, M.E., Lohmann, K.C, Hernán, J., Quijada, E., Suárez, P., & Omodeo-Salé, S. (2011). Evolution of an intra-plate rift basin: the Latest Jurassic–Early Cretaceous Cameros Basin (Northwest Iberian Ranges, North Spain). In L. Pomar, and C. Arenas, (Eds.), *Geo-Guías* (8) (pp. 119-154), Post-Meeting field trips, 28th International Association of Sedimentologists, Sociedad Geológica de España.

McIlroy, D., Flint, S., Howell, J.A., & Timms, N. (2005). Sedimentology of the tide-dominated Jurassic Lajas Formation, Neuquén Basin, Argentina. In G.D., Veiga, L.A., Spalletti, J.A., Howell, and E., Schwartz, (Eds.), *The Neuquén Basin, Argentina: A Case Study in*

Sequence Stratigraphy and Basin Dynamics (pp. 83–107). London: Geological Society of London, Special Publication, 252.

Mendelssohn, I.A., & Batzer, D.P. (2006). Abiotic constraints for wetland plants and animals. In D.P., Batzer, and R.R., Sharitz, (Eds.), *Ecology of Freshwater and Estuarine Wetlands* (pp. 82–114). Berkeley: University of California Press.

Miall, A.D. (2010). Alluvial Deposits. In N.P., James, and R.W., Dalrymple, (Eds.), *Facies Models 4* (pp. 105–138). St. John's, Newfoundland: Geological Association of Canada.

Millward, D., Davies, S.J., Williamson, F., Curtis, R., Kearsey, T.I., Bennett, C.E., Marshall, J.E.A., Browne, M.A.E. (2018) Early Mississippian evaporites of coastal tropical wetlands. *Sedimentology*, doi: 10.1111/sed.12465

Nio, S.D., & Yang, C.H. (1991). Diagnostic attributes of clastic tidal deposits: a review. In D.G., Smith, G.F., Reinson, B.A., Zaitlin, and R.A., Rahmani, (Eds.), *Clastic Tidal Sedimentology* (pp. 3–28). C Canadian Society of Petroleum Geologists, Memoir 16.

Norman, ME. (1974). Improved techniques for selective staining of feldspar and other minerals using amaranth. *US Geological Survey, Journal Research*, 2, 73-79.

Ogg, J.G., Ogg, G., & Gradstein, F.M. (2008). *The Concise Geologic Time Scale*. Cambridge: Cambridge University Press, p. 177.

Ogg, J.G., Hinnov, L.A., & Huang, C. (2012) Cretaceous. In F.M., Gradstein, J.G., Ogg, M.D., Ogg, and G. M., Schmitz, (Eds.), *The geologic time scale* (pp. 793-853). Amsterdam: Elsevier.

Omodeo-Salé, S., Guimerà, J., Arribas, J., & Mas, R. (2014). Tectono-stratigraphic evolution of an inverted extensional basin: the Cameros Basin (north of Spain). *International Journal of Earth Sciences*, 103, 1597–1620.

Pascual-Arribas, C., Sanz-Pérez, E., Hernández-Medrazo, N., & Latorre Macarrón, P. (2007). Lepidotes sp. en la aloformación Valdeprado del Cretácico Inferior (Berriasiense) de la Cuenca de Cameros (Cordillera Ibérica, Soria, España). *Studia Geologica Salmanticensia*, 43 (2), 193–206.

Pestrong, R. (1972). Tidal flat sedimentation at Cooley Landing southwest San Francisco Bay. *Sedimentary Geology*, 8, 251-288.

Platt, N. H. (1989)a. Continental sedimentation in an evolving rift basin: the Lower Cretaceous of the western Cameros Basin (northern Spain). *Sedimentary Geology*, 64, 91-109.

Platt, N. H. (1989)b. Lacustrine carbonates and pedogenesis: sedimentology and origin of palustrine deposits from the Early Cretaceous Rupelo Formation, W Cameros Basin, N Spain. *Sedimentology*, 36, 665-684.

Platt, N. H. (1990). Basin evolution and fault reactivation in the western Cameros basin, Northern Spain. *Geological Society of London, Journal*, 147, 165-175.

Platt, N. H. (1994). The western Cameros Basin, northern Spain: Rupelo Formation (Berriasian). In E., Gierlowky-Kordesh, and K., Kelts, (Edts.) *Global Geological Record of Lake Basins, v. 1* (pp.195-202). Cambridge: Cambridge University Press.

Platt, N.H. (1995). Sedimentation and tectonics of a syn-rift succession: Upper Jurassic alluvial fans and palaeokarst at the late Cimmerian unconformity, Western Cameros Basin, northern Spain. In G., Plint, (Ed.), *Sedimentary Facies Analysis* (pp. 219-236). Oxford: International Association of Sedimentologists, Special Publication, 22, Blackwell Science.

Platt, N.H., & Pujalte, V. (1994). Correlation of Upper Jurassic-Lower Cretaceous continental sequences from the southern Biscay margin, northern Spain. *Geological Society of London, Journal*, 151, 715-726.

Platt, N.H., & Wright, V.P. (1991). Lacustrine carbonates: facies models, facies distributions and hydrocarbon aspects. In P., Anadón, L., Cabrera, and K., Kelts (Eds.), *Lacustrine Facies Analysis* (pp. 57–74). Oxford: International Association of Sedimentologists, Special Publication, 13, Blackwell Science.

Pujalte, V. (1982). Tránsito Jurásico-Cretácico, Berriasiense, Valanginiense, Hauteriviense y Barremiense. In A., García (Ed.), *El Cretácico de España* (pp. 51-63). Madrid: Universidad Complutense de Madrid.

Pujalte, V., Robles, J.C., García-Ramos, J.C., & Hernández, J.M. (2004). El Malm - Barremiense no marinos en la Cordillera Cantábrica. In J.A., Vera (Ed.), *Geología de España* (pp. 288-291). Madrid: Sociedad Geológica de España - Instituto Geológico y Minero de España.

Quijada, I.E., Suarez-Gonzalez, P., Benito, M.I., & Mas, R. (2013)a. New insights on stratigraphy and sedimentology of the Oncala Group (eastern Cameros Basin): implications for the paleogeographic reconstruction of NE Iberia at Berriasian times. *Journal of Iberian Geology*, 39, 313–334.

Quijada, I.E., Suarez-Gonzalez, P., Benito, M.I., & Mas, R. (2013)b. Depositional depth of laminated carbonate deposits: Insights from the Lower Cretaceous Valdeprado Formation (Cameros Basin, Northern Spain). *Journal of Sedimentary Research*, 83, 241-257.

Quijada, I.E., Suarez-Gonzalez, P., Benito, M.I., Lugli, S., & Mas, R. (2014). From carbonate-sulphate interbeds to carbonate breccias: The role of tectonic deformation and diagenetic processes (Cameros Basin, Lower Cretaceous, N Spain). *Sedimentary Geology*, 312, 76-98.

Quijada, I.E, Suarez-Gonzalez, P., Benito, M.I., & Mas, R. (2016)a. Tidal versus continental sandy_muddy flat deposits: Evidence_from_the Oncala Group (Early Cretaceous, N Spain). In B, Tessier, and J.Y., Reynaud (Eds.), *Contributions to Modern and Ancient Tidal Sedimentology: Proceedings of the Tidalites 2012 Conference* (pp. 133-159). Chichester, West Sussex: International Association of Sedimentologists, Special Publication 47, Wiley Blackwell.

Quijada, I.E., Suarez-Gonzalez, P., Benito, M.I., & Mas, R. (2016)b. Los isótopos de S en los yesos del Grupo Oncala: evidencia de influencia marina en los depósitos carbonático-evaporíticos berriasienses de la cuenca de Cameros (La Rioja-Soria). *Geo-Temas*, 16, 555-558.

Ramsar Convention (2002). Principles and guidelines for incorporating wetland issues into Integrated Coastal Zone Management (ICZM), Resolution VIII.4 (2002), 8th Meeting of the Conference of the Contracting Parties to the Convention on Wetlands, http://www.ramsar.org/sites/default/files/documents/pdf/res/key_res_viii_04_e.pdf.

Reineck, H.E. (1972). Tidal flats. In J. K., Rigby, and W. K., Hamblin (Eds.), *Recognition of Ancient Sedimentary Environments* (pp. 146 -159). Tulsa: SEPM, Special Publication 16.

Reineck, H.E., & Wunderlich, F. (1968). Classification and origin of flaser and lenticular bedding. *Sedimentology*, 11, 99–104.

Sacristán-Horcajada, S., Mas, J.R., & Arribas, M.E. (2012)a. Evolución de los sistemas lacustres asociados al estadio temprano de rift en el Semigraben de Rupelo (NO de la Cuenca de Cameros, España): subsidencia e influencia marina. *Geo-temas*, 13, 89-92.

Sacristán-Horcajada, S., Mas, J.R., & Arribas, M.E. (2012)b. Marine influence in the third depositional sequence (Lower-middle Berriasian) of the mainly continental synrift sedimentary record in the western Cameros Basin, (N Spain). Abstractbook, 29th IAS Meeting of Sedimentology 2012, Schladming, Austria.

Sacristán-Horcajada, S., Arribas, M.E., & Mas, J.R. (2012)c. Tipo e intensidad de los procesos pedogenéticos en los sedimentos aluviales y lacustres de la primera secuencia de depósito del Semigraben de Rupelo. *Geo-Temas*, 13, 112-115.

Sacristán-Horcajada, S., Mas, R., & Arribas, M.E. (2015). Early syn-rift evolution in the W Cameros Basin (Upper Jurassic, NW Iberian Range) Spain. *Journal of Sedimentary Research*, 85, 794–819.

Sacristán-Horcajada, S., Arribas, M.E., & Mas, R. (2016). Pedogenetic calcretes in early syn-rift alluvial systems (Upper Jurassic, West Cameros Basin), Northern Spain. *Journal of Sedimentary Research*, 86, 794–819.

Salas, R., Guimerà, J., Mas, R., Martín-Closas, C., Meléndez, A., & Alonso, A. (2001). Evolution of the Mesozoic Central Iberian Rift System and its Cainozoic inversion (Iberian chain). In P.A., Ziegler, W., Cavazza, A.H.F., Robertson, S., Crasquin-Soleau (Eds.), Peri-Tethys Memoir 6: Peri-Tethyan Rift/Wrench Basins and Passive Margins (pp. 145–186). Paris: Mémoires du Museum National d'Histoire Naturelle, 186.

Salomon, J. (1982). El Cretácico inferior de Cameros-Castilla. In A., García (Ed.), *El Cretacico de España* (pp. 345-387). Madrid: Universidad Complutense de Madrid.

Schudack, M. (1987). Charophytenflora und fazielle Entwicklung der Grenzschichten mariner Jura/Wealden in den Nordwestlichen Iberischen Ketten (mit Vergleichen zu Asturien und Kantabrien). *Palaeontographica . Abt*. B, 204, 108 p.

Schudack, U. & Schudack, M. (2009). Ostracod biostratigraphy in the Lower Cretaceous of the Iberian Chain (eastern Spain). *Journal of Iberian Geology*, 35, 141-168.

Schudack, U. & Schudack, M. (2012). Non-Cypridean Ostracoda from the Lower Cretaceous of the Iberian Chain (Spain). *Neues Jahrbuch für Geologie und Paläontologie*, 266 (3), 251–271.

Semeniuk V. (1981). Sedimentology and the stratigraphic sequence of a tropical tidal flat, northwestern Australia. *Sedimentary Geology*, 29, 195-221.

Suarez-Gonzalez, P., Quijada, I.E., Benito, M.I., & Mas, J.R. (2013). Eustatic versus tectonic control in an intraplate rift basin (Leza Fm, Cameros Basin). Chronostratigraphic and paleogeographic implications for the Aptian of Iberia. *Journal of Iberian Geology*, 39, 285–312.

Suarez-Gonzalez, P., Quijada, I.E., Benito, M.I., Mas, J.R., Merinero, R., & Riding, R. (2014). Origin and significance of lamination in Lower Cretaceous stromatolites and proposal for a quantitative approach. *Sedimentary Geology*, 300, 11-27.

Suarez-Gonzalez, P., Quijada, I.E., Benito, M.I., & Mas, R. (2015). Sedimentology of ancient coastal wetlands: Insights from a Cretaceous multifaceted depositional system. *Journal of Sedimentary Research*, 85, 95-117.

Suarez-Gonzalez, P., Quijada, I.E., Benito, M.I., & Mas, R. (2016)a. Do stromatolites need tides to trap ooids? Insights from a Cretaceous system of coastal-wetlands. In B., Tessier, and J.Y., Reynaud (Eds.). *Contributions to Modern and Ancient Tidal Sedimentology*. *Proceedings of the Tidalites 2012 Conference* (pp. 161-190).. Chichester, West Sussex: International Association of Sedimentologists, Special Publication 47, Wiley Blackwell.

Suarez-Gonzalez, P., Benito, M.I., Mas, R., Quijada, I.E., & Campos-Soto, S. (2016)b. Influencia del Keuper y de la estructuración tardivarisca en la arquitectura de las unidades sin-extensionales del borde norte de la Cuenca de Cameros. *Geotemas*, 16, 185-188.

Tessier, B. (1993). Upper intertidal rhythmites in the Mont-Saint-Michel Bay (NW France): Perspectives for paleoreconstruction. *Marine Geology*, 110, 355-367.

Thompson, R.W. (1968). *Tidal flat sedimentation on the Colorado River Delta northwest Gulf of California*. Geological Society of American Memoir 107, 133 p.

Torcida Fernández-Baldor, F., Díaz-Matínez, I., Contreras, R., Huerta, P., Montero, D., & Urién, V. (2015). Unusual sauropod tracks in the Jurassic-Cretaceous interval of the Cameros Basin (Burgos, Spain). *Journal of Iberian Geology*, 41 (1), 141-154.

Tugend, J., Manatschal, G., Kusznir, N.J., Masini, E., Mohn, G., & Thinon, I. (2014). Formation and deformation of hyperextended rift systems: Insights from rift domain mapping in the Bay of Biscay-Pyrenees. *Tectonics*, doi: 10.1002/2014TC003529

Tugend, J., Manatschal, G., & Kusznir, N.J. (2015). Spatial and temporal evolution of hyperextended rift systems: Implication for the nature, kinematics, and timing of the Iberian-European plate boundary. *Geology*, 43, 15-18.

Vakhrameev, V. A. (1991). *Jurassic and Cretaceous floras and climates of the Earth*. Cambridge: Cambridge University Press, 318 p.

Vegas, R., & Banda, E. (1982). Tectonic framework and Alpine evolution of the Iberian Peninsula. *Earth Evolution Sciences*, 4, 320-343.

Warren, J.K. (2016). *Evaporites: A geological compendium*. Springer, Cham, 1813 pp.

Weissmann, G.S., Hartley, A.J., Nichols, G.J., Scuderi, L.A., Olson, M., Buehler, H., and Banteah, R. (2010). Fluvial form in modern continental sedimentary basins: Distributive fluvial systems. *Geology*, 38, 39-42.

Wilkinson, B.H. & Drummond, C.N. (2004) Facies mosaics across the Persian Gulf and around Antigua: stochastic and deterministic products of shallow-water sediment accumulation. *Journal of Sedimentary Research*, 74, 513–526.

Wolanski, E., Brinson, M.M., Cahoon, D.R., & Perillo, G.M.E. (2009). Coastal wetlands: a synthesis. In G.M.E., Perillo, E., Wolanksi, D.R., Cahoon, and M.M., Brinson (Eds.), *Coastal Wetlands* (pp. 1–62). Amsterdam: Elsevier.

Ziegler, A. M., Parrish, J.M., Jiping, Y., Gyllenhaal, E. D., Rowley, D. B., Parrish, J. T., Shangyou, N. Bekker, A., & Hulver, M. L. (1993) Early Mesozoic Phytogeography and Climate. Philosophical Transactions. *Biological Sciences*, 341, 297-305.

FIGURE CAPTIONS

Figure 1: A) The Cameros Basin (Cm) in the geological setting of the Iberian Peninsula, showing its location in relation to the two main Mesozoic intraplate extensional systems of the plate: the Basque-Cantabrian Basins Extensional System (BCB) and the Iberian Basins Extensional System (IB) (modified from Mas et al., 2004). B) Major cycles or megasequences in the Cameros area of the Basin Iberian Basins Extensional System (IB) (modified from Mas el al. 2011).

Figure 2: A) Geological map of the Cameros Basin (modified from Mas et al. 2002, 2003) showing the location of the geological cross sections of Fig. 2B and the studied area (shown in detail in Fig. 2C). B) Geological cross sections of the Cameros Basin (1 - 1´, 2 - 2´ and 3 - 3´) (modified from Guimerà et al. 1995, and Mas et al. 2003). C) Geological map of the West Cameros Basin (modified from Mas et al. 2002, 2003) showing the location of the stratigraphic sections in this work [Arlanzón (AZ), Torrelara (TO), Paules (PA), Aceña (AC), Morrión (MO), Rupelo (RU), San Millán (SM), Cubillejo (CU), Quintanilla (QU), Campolara (CA), Hortigüela (HO), Vizcainos (VZ), Jaramillo Quemado (JQ), Pinilla de los Moros (PM), Castrovido (CTV), Terrazas 2 (TR2), Terrazas 1 (TR1), Moncalvillo (MN), Arroyo del Helechal (AHE), Mamolar Norte (MAN), Mamolar Sur (MAS), Pinilla de los Barruecos (PI), La Gallega Sur (GAS), Talveila (TAL), Doña Santos (DS), Camino Forestal (CF), Área Recreativa (AR), Brezales (BR) and Espejón (ES)]. See cross correlations in Fig. 5 (A-A´, B-B´and C-C´).

Figure 3: A) General stratigraphic record of the Cameros Basin (modified from Mas et al. 2004, 2011); DS, depositional sequences (1 - 8); red rectangle indicates the Tithonian – Berriasian stratigraphic record in the studied sector. B) Stratigraphic framework of the sedimentary record of the W Cameros Basin (modified from Arribas et al. 2003); the red rectangle indicates the focus depositional sequence (DS 3).

Figure 4: Thickness distribution of the Tithonian – Berriasian formations in the study sections. A) Brezales Fm (DS 1); B) Boleras Fm (DS 1); C) Jaramillo Fm (DS 2); D) Campolara Fm (DS 2); E) Salcedal Fm (DS 3); F) San Marcos Fm (DS 3). The size of the black circles is directly proportional to the thickness in each section (also expressed numerically). Cross-correlations A – A' and B – B' (in Fig. 2C,

Fig. 4, and Fig. 5) for the stratigraphic sections of the North Sector of the West Cameros Basin, and cross-correlation C – C'(in Fig. 2C, Fig. 4, Fig. 5) for sections of its South Sector.

Figure 5: Cross-correlations (A – A', B – B', and C – C') showing the distribution of the depositional sequences (DS 1, DS 2, and DS 3) and their corresponding formations. Cross-correlations A – A' and B – B' (Fig. 2C, Fig. 4, and Fig. 5) for the stratigraphic sections of the North Sector of the West Cameros Basin, and cross-correlation C – C'(Fig. 2C, Fig. 4, Fig. 5) of its south sector.

Figure 6: Representative stratigraphic sections of the facies recorded in the third depositional sequence (DS 3) of the Tithonian-Berriasian record. *Upper part*: Sections located in cross-correlation A – A' (Fig. 2C, Fig. 4, and Fig. 5) and Arlanzón section. *Lower part*: Sections located in cross-correlation B – B' (Fig. 2C, Fig. 4, and Fig. 5).

Figure 7: Architectural elements and facies associations (FA) distinguished in the third depositional sequence (DS 3) of the Tithonian-Berriasian record in the study area. The letters of facies in each FA refer to the lithofacies described in Table 2. Legend as in Fig. 6.

Figure 8: Field photographs of facies and facies associations. A) Fluvial paleo-channel (CH) with lateral accretion (LA) and floodplain fines (FF) in FA-1, Salcedal Fm, CTV section. B) Siliciclastic tidal flat facies (Srf and Fm) in FA-2, Salcedal Fm, CTV section. C) Lbf, and Mr facies of FA-3, interpreted as having been deposited in marine-influenced water bodies, San Marcos Fm, RU section. D) Desiccation cracks on top of Lbf facies of FA-3 deposits (marine-influenced water bodies), San Marcos Fm, RU section. E) Lb, and Mr facies of FA-4, interpreted as deposits of water bodies with no to very little marine-influence, San Marcos Fm, SM section (arrow length 3 m). F) Detail of fish scale in FA-4, San Marcos Fm, RU section. G) Detail of fish teeth in FA-4, San Marcos Fm, SM section. H) Sequences of FA-5 facies (deposits of marine-influenced water bodies to palustrine settings) overlying FA-6, San Marcos Fm, CA section (arrow length 7 m). I) Dinosaur footprints on palustrine carbonates (Ln) on top of FA-6, San Marcos Fm, QU section (small wall height 0.6 m approx.).

Figure 9: Microscopic character of facies and components. A) Wackestone with miliolid foraminifera and ostracods, Lbf facies in FA-3, San Marcos Fm, RU section. B) Wackestone with ostracod valves showing “cup-in-cup” arrangement and miliolid foraminifera, Lbf facies in FA-3, San Marcos Fm, RU section. C) Detail of a miliolid section, Lbf facies in FA-3, San Marcos Fm, RU section. D) and E) Wackestone with minute foraminifera (white arrows) and ostracods, Lbf facies in FA-3, San Marcos Fm, AZ section. F) Calcite pseudomorphs (white arrows) after evaporite crystals (lenticular gypsum?) within a dolomicrite matrix, Lbf facies in FA-3, San Marcos Fm, RU section. G) Wackestone with ostracods, Lb facies in FA-4, San Marcos Fm, RU section. H) Wackestone - packstone with ostracods and micritic nodular-brecciated structure, Lb facies in FA-4, San Marcos Fm, RU section. I) Wackestone – packstone with ostracods, Lb facies in FA-4, San Marcos Fm, RU section.

Figure 10: Microscopic character of facies and components. A) and B) Detailed section of a specimen of dasycladales, Lmd facies in FA-5, San Marcos Fm, HO section. C) Wackestone with dasycladales, charophytes and ostracods, Lmd facies in FA-5, San Marcos Fm, HO section. D) Detailed section of a charopyte thallus, Lmd facies in FA-5, San Marcos Fm, HO section. E) Alveolar (rhizoliths) and clotted microfabrics in a pedogenetic calcrete, Ln in FA-6, San Marcos Fm, PA section. F) Peloidal wackestone – packstone with charophytes and ostracods, Lm facies in FA-6, San Marcos Fm, HO section. G) Mudstone - wackestone with peloids, ostracods and charophytes, Lm facies in FA-6, San Marcos Fm, CA section. H) Calcite pseudomorphs (white arrows) after evaporite crystals (probable gypsum) in a carbonate nodule and within the micrite matrix, Ln in FA-6, San Marcos Fm, PA section.

Figure 11: Schematic interpretive framework of the facies associations and depositional environments during maximum marine influence of the San Marcos Fm. This framework is based on the correlation of the stratigraphic sections of the cross-sections A – A’ and B – B’ (see their locations in Figures 2C, 4, 5, and 6).

Figure 12: Schematic map of the study area (W Cameros Basin) showing the distribution of stratigraphic sections recording the third depositional sequence (DS 3; white circles in the rectangle-framed area), and also showing the main paleo-faults that may have controlled the sedimentation in the western sector of the “Cameros tectonic Unit” (*sensu* Mas et al. 2002, 2003).

Figure 13: Interpretive paleogeographic distribution and evolution of the study area (location shown by the rectangle-framed area of Fig. 12) during deposition of the San Marcos Fm. A) Schematic paleogeography during the lacustrine - palustrine stage in the north sector and Arlanzón area. B) Schematic paleogeography during a subsequent coastal wetlands stage of maximum marine influence ("Berriasian transgressive stage") in the north sector and Arlanzón area.

Figure 14: Paleogeographic reconstruction during the "Berriasian transgression" (Lower – Middle? Berriasian) in the extensional basins of the Iberian Plate (North and East of Iberia). These features are indicated showing the location and main facies of Berriasian deposits in the North and East of the Iberian Peninsula. BC = Basque-Cantabrian Basin (*NCP* = Norcastilian Platform, *NCT* = Navarrese – Cantabrian Trough, BA = Basque Arch); WC = West Cameros Basin; EC = East Cameros Basin; CI = Central Iberian Range; SI = South Iberian Basin; WM = West Maestrat Basin; EM = East Maestrat Basin; CC = Catalonian Coastal Ranges; P = Pyrenean Basin (modified from Quijada et al. 2013a).

Figure 15: Reconstruction of the Upper Jurassic - Lower Cretaceous paleotectonic setting along the Iberian-European plate boundary when the maximum extent of Berriasian transgression reached the Cameros Basin from the north. BoBP = Bay of Biscay – Parentis rift system, PBC = Pyrenean - Basque-Cantabrian rift systems; IB = Iberian intraplate extensional basins system, *CC* = Catalonian Coastal Ranges (modified from Tugend et al. 2015).

Table 1. Stratigraphy and general characteristics of the Tithonian - Berriasian depositional sequences (DS 1, DS 2 and DS 3) in the W Cameros Basin. (***** This study - see DS 3 Formations). For brevity, throughout this article, the authors have used the names of the Tithonian - Berriasian Formations in their shortest form: Brezales Fm (Señora de Brezales Fm), Boleras Fm, Jaramillo Fm (Jaramillo de la Fuente Fm), Campolara Fm, Salcedal Fm (Río del Salcedal Fm), and San Marcos Fm (Río de San Marcos Fm).

Table 2. DS 3 Lithofacies (siliciclastic facies code follows Miall 2010).

Table

Click here to access/download;Table;Table_1_Mas-et-al_JIG_WORD.pdf

Table 1. Stratigraphy and general characteristics of the Tithonian **-** Berriasian Depositional Sequences (DS 1, DS 2 and DS 3) in the West Cameros Basin. (***** This study - see DS 3 Fms).

Depositional Sequences	Age	Formations. General characteristics.
DS 3	**Tithonian ------ Lower to middle Berriasian------**	**Río de San Marcos Fm** (also **San Marcos Fm**). – The San Marcos Fm is 0 to 84 m thick and consists of limestone (mainly mudstone and wackestone), often silty, well-bedded, and alternating with marl. Its fossil content consists of ostracods, charophytes, benthic foraminifers (mainly miliolids), dasycladales*****, fish remains, gastropods and bivalves. It corresponds to a carbonate coastal wetland***** depositional system. The Pinilla de los Moros Fm (DS 6.1, Hauterivian – Barremian aged) unconformable lies on this Formation (Fig. 5).
DS 3	**Tithonian ------ Lower to middle Berriasian------**	**Río del Salcedal Fm** (also **Salcedal Fm**). – The Salcedal Fm is 0 to 69 m thick and consists mainly of lenticular bodies of sandstone, and silty and sandy mudstone, and in its uppermost part thin alternating sheets of flaser-bedded sandstone and silty mudstone*****. It corresponds mainly to a meandering fluvial system, and its uppermost part to a siliciclastic tidal flat***** that fringed the fluvial system. It changes gradually both vertically and laterally into the San Marcos Fm.
DS 2	**Tithonian ------ Lower to middle Berriasian------**	**Campolara Fm**. – The Campolara Fm is 0 to 56 m thick and consists of limestone (mudstone, wackestone and packstone), often nodular, and marl, displaying paleosols, with charophytes, ostracodes, and gastropods. It corresponds to shallow lacustrine to palustrine depositional systems.
DS 2	**Tithonian ------ Lower to middle Berriasian------**	**Jaramillo de la Fuente Fm** (also **Jaramillo Fm**). - The Jaramillo Fm is 0 to 380m thick and consists of lenticular bodies of sandstone, silty and sandy mudstone, and some intercalations of limestone interpreted as deposited in a fluvial system with meandering channels, traversing clayey floodplains with zones of shallow ephemeral lakes. It changes gradually both vertically and laterally into the Campolara Fm.
DS 1	**Tithonian ------ Lower to middle Berriasian------**	**Boleras Fm**. - The Boleras Fm is 0 to 116 m thick and consists of limestones (mudstone, wackestone, and packstone) with charophytes, ostracods, gastropods, and bivalves. Being interpreted as deposited in lacustrine – palustrine systems. Pedogenic modifications (pedogenic calcretes) are characteristic. In the South Sector (Fig.2C, Fig. 5), the Peñacoba Fm (DS 5, Valanginian – Hauterivian, NW area of the South Sector) or the Pinilla de los Moros Fm (DS 6.1, Hauterivian – Barremian, SE area of the South Sector) unconformable overlie on DS 1. These Fms overlie the Boleras Fm, or if the latter is absent, the Brezales Fm.
DS 1	**Tithonian ------ Lower to middle Berriasian------**	**Señora de Brezales Fm** (also Nuestra Señora de Brezales Fm and **Brezales Fm**). - The Brezales Fm overlies a major unconformity that developed on pre-rift marine Callovian to Kimmeridgian sandstones and limestones. In the North and Central sectors of the West Cameros Basin (Fig.2C, Fig. 5); this unconformity developed over the Callovian limestones and sandy limestones (Pozalmuro Fm, defined by Wilde 1990). In the south sector of the study area, the unconformity developed over the Middle–Upper Jurassic sandstones and conglomerates. The Brezales Fm is 0 to 222 m thick and consists of conglomerates, sandstones, sandy mudstones, and sandy limestones deposited in alluvial systems (alluvial and fluvial fans). Pedogenic modifications (pedogenic calcretes) are common. It changes gradually both vertically and laterally into the Boleras Fm.

Table

Click here to access/download;Table;Table_2_Mas-et-al_JIG_WORD.pdf

Table 2. DS 3 Lithofacies (siliciclastic facies code follows Miall, 2010).

Facies code	Lithofacies	Sedimentary structures or textural organization and microfabrics	Interpretation
Siliciclastic lithofacies			
St	sandstone (subarkose), fine to coarse grained	solitary or grouped trough crossbeds	sinuous-crested and linguoid (3-D) dunes
Sr	sandstone (subarkose), very fine to fine grained	ripple cross-lamination (occasionally climbing)	ripples (lower flow regime)
Srf	sandstone (subarkose), very fine to fine grained and thin interbedded dark grey siliciclastic mudstone	flaser bedding	mud-draped current and wave ripples; alternating bed-load traction and suspended-load settling; tidal?
Sh	sandstone (subarkose), very fine to medium grained	horizontal lamination, parting or streaming lineation	plane-bed flow (super-critical flow)
Fm	siliciclastic mudstone; occasionally sandy or marly siltstone; usually reddish and occasionally dark grey	massive, desiccation cracks, roots traces, bioturbation, carbonate nodules; occasionally ripple cross-laminated thin layers intercalated	overbank, root bed, incipient soil; occasionally ripples (lower flow regime)
Carbonate and mixed carbonate-siliciclastic lithofacies			
Lb	well-bedded marly limestone, sometimes dolomitic; abundant ostracods, some charophytes, and fish scales and teeth	marly wackestone-mudstone, packstone, occasionally dolomitic; common clotted-peloidal microfabrics; locally gypsum pseudomorphs; unfragmented microfossils; desiccation cracks, bioturbation, no pedogenic features	carbonate (partly microbialitic) and mixed carbonate-siliciclastic muddy sediment deposited in a quiet, shallow water body with none or very little marine influence
Lbf	well-bedded marly limestone, sometimes dolomitic; ostracods, benthic foraminifera, occasional charophytes, and fish scales and teeth	marly wackestone-mudstone, packstone, occasionally dolomitic; common clotted-peloidal microfabrics; locally gypsum pseudomorphs; unfragmented microfossils; desiccation cracks, bioturbation, no pedogenic features	carbonate (partly microbialitic) and mixed carbonate-siliciclastic muddy sediment deposited in a quiet, shallow coastal marine-influenced water body
Lm	massive limestone, generally marly; charophytes (gyrogonites and thalli), ostracods, gastropods, bivalves; occasionally oncoliths and dinosaur foot prints	mudstone, wackestone, commonly marly; common clotted-peloidal microfabrics; very rare gypsum pseudomorphs; bioturbation, subaerial exposure, especially desiccation cracks	muddy carbonate sediment (partly microbialitic) deposited in a shallow, quiet water body with none or very little marine influence
Lmd	massive limestone, generally marly; charophytes (gyrogonites and thalli), filamentous calcimicrobes, ostracods, dasycladales, scarce benthic foraminifera, gastropods, bivalves	mudstone, wackestone, commonly marly; common clotted-peloidal and filamentous microfabrics; bioturbation, subaerial exposure, especially desiccation	muddy carbonate sediment (partly microbialitic) deposited in a shallow, quiet, and brackish coastal marine-influenced water body
Ln	nodular limestone, intraclasts, black pebbles; scarce charophytes, ostracods, gastropods, bivalves	original textures rarely preserved, intense pedogenic modification (desiccated, brecciated and nodular microfabrics)	carbonate sediment deposited in shallow water bodies with none or very little marine influence and palustrine environments affected by periodical desiccation and pedogenesis
Mr	massive marl and muddy-silty limestone; ostracods, charophytes, fish scales and teeth; usually dark gray	marl and marly mudstone, fines siliciclastic and muddy carbonate; bioturbation and occasionally carbonate nodules, calcretes, root traces	siliciclastic - carbonate muddy sediment deposited in quiet, shallow, water bodies both with no or very little marine influence and with marine influence; locally moderate to intense pedogenic features linked to sub-aerial exposure
P	paleosol carbonate (pedogenic calcrete)	pedogenic microfabric and features: filaments, mootling, desiccation, nodules, lamination, brecciation, pseudomicrokarst cavities, pedotubules, rhizocretions	pedogenic secondary carbonate displacive precipitation

Figure
Click here to access/download;Figure;Fig_01_Mas-et-al_JIG_REV.pdf

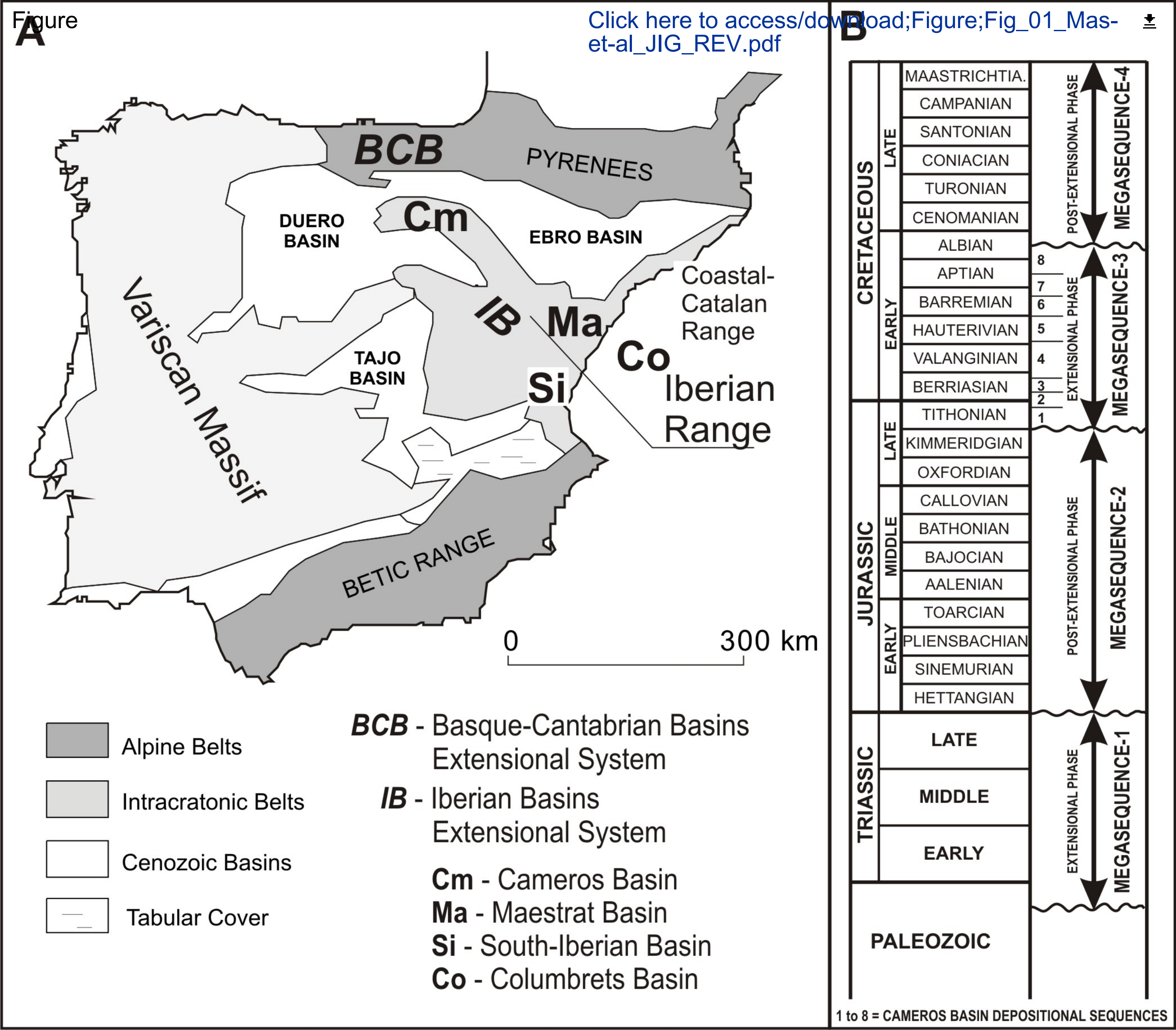

Figure
Click here to access/download;Figure;Fig_02_Mas-et-al_JIG_PDF.pdf

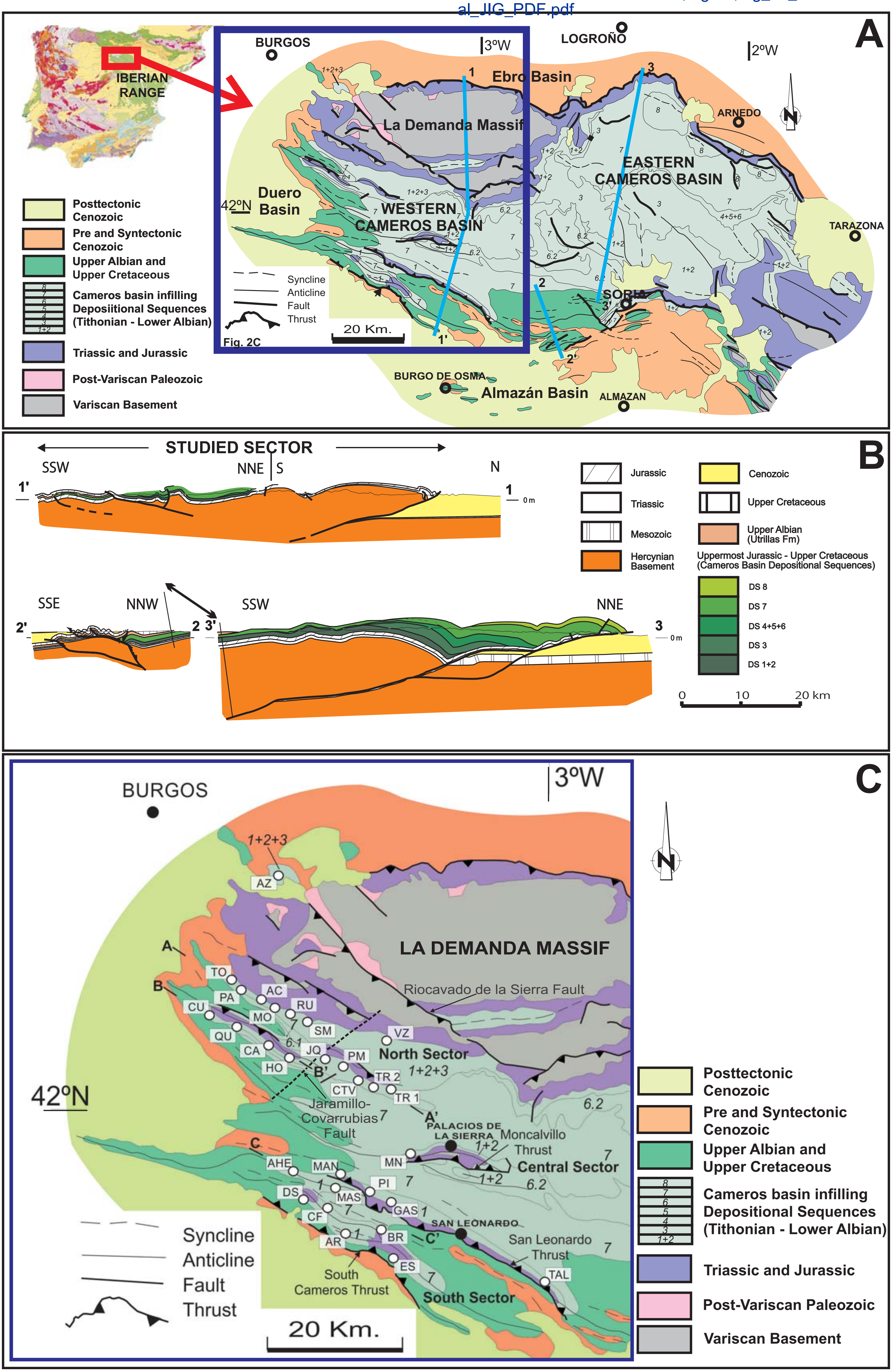

Figure
Click here to access/download;Figure;Fig_03_Mas-et-al_JIG_PDF.pdf

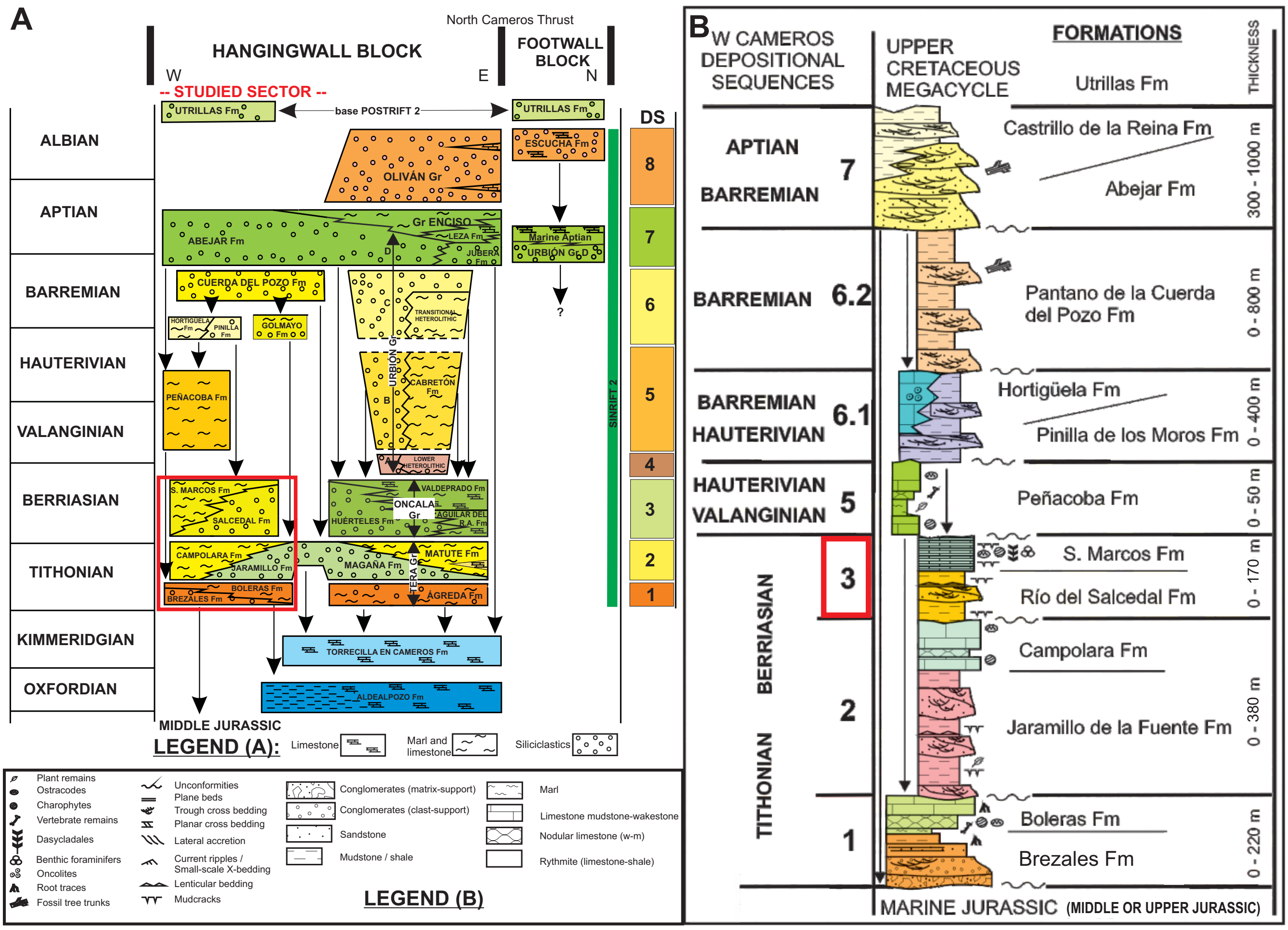

Figure
Click here to access/download;Figure;Fig_04_Mas-et-al_JIG_PDF.pdf

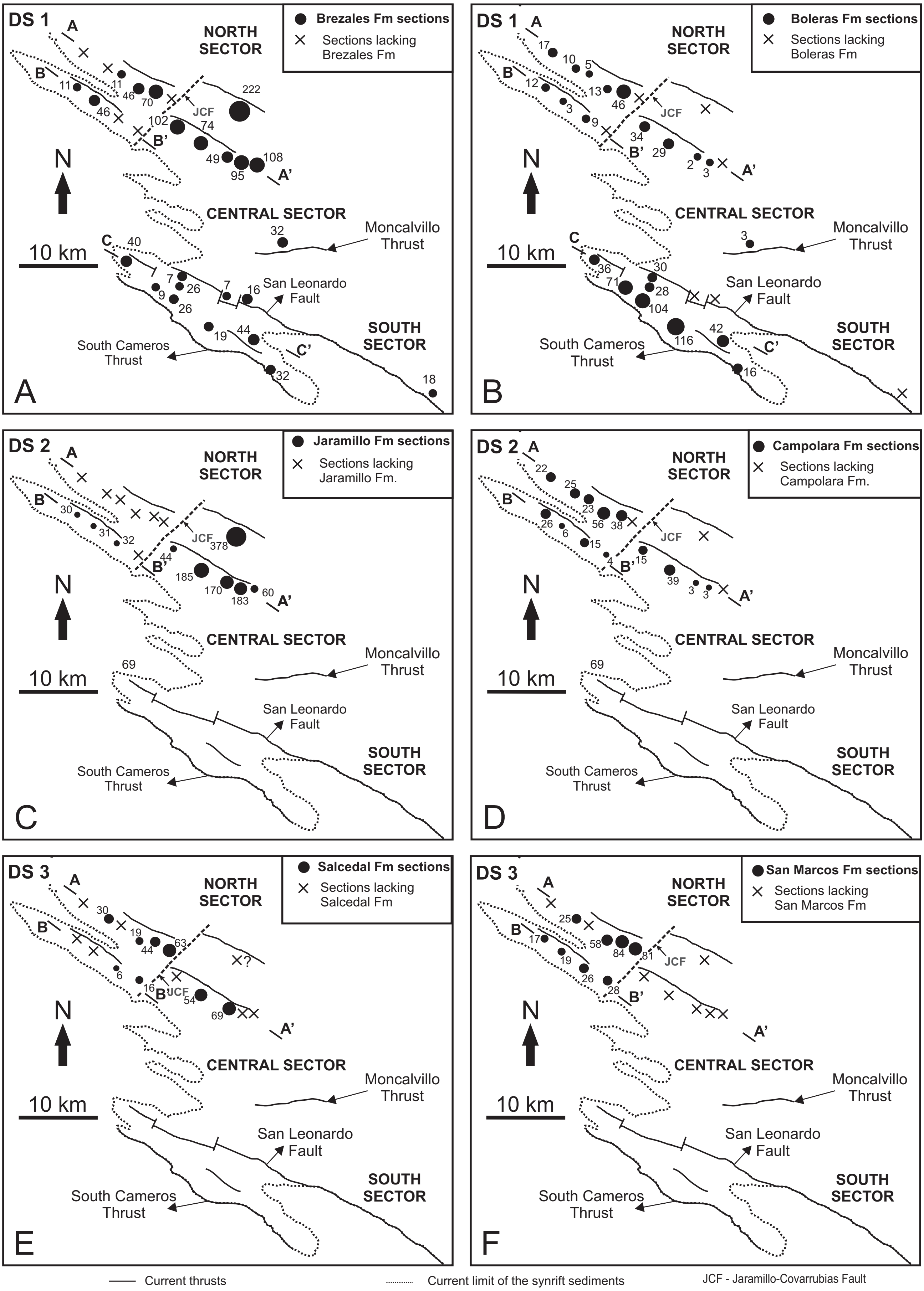

Click here to access/download;Figure;Fig_05_Mas-et-al_JIG_PDF.pdf

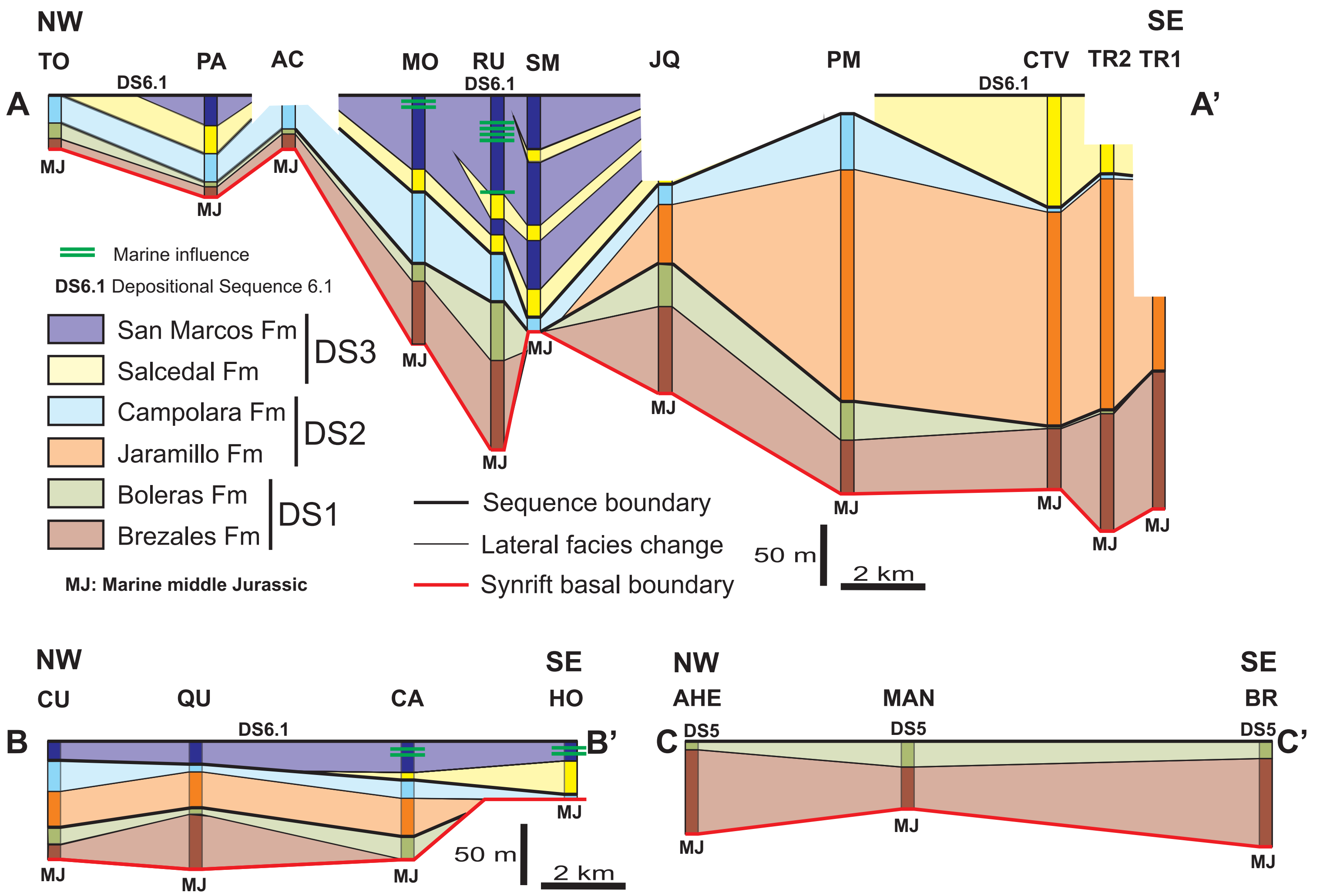

Figure
Click here to access/download;Figure;Fig_06_Mas-et-al_JIG_PDF.pdf

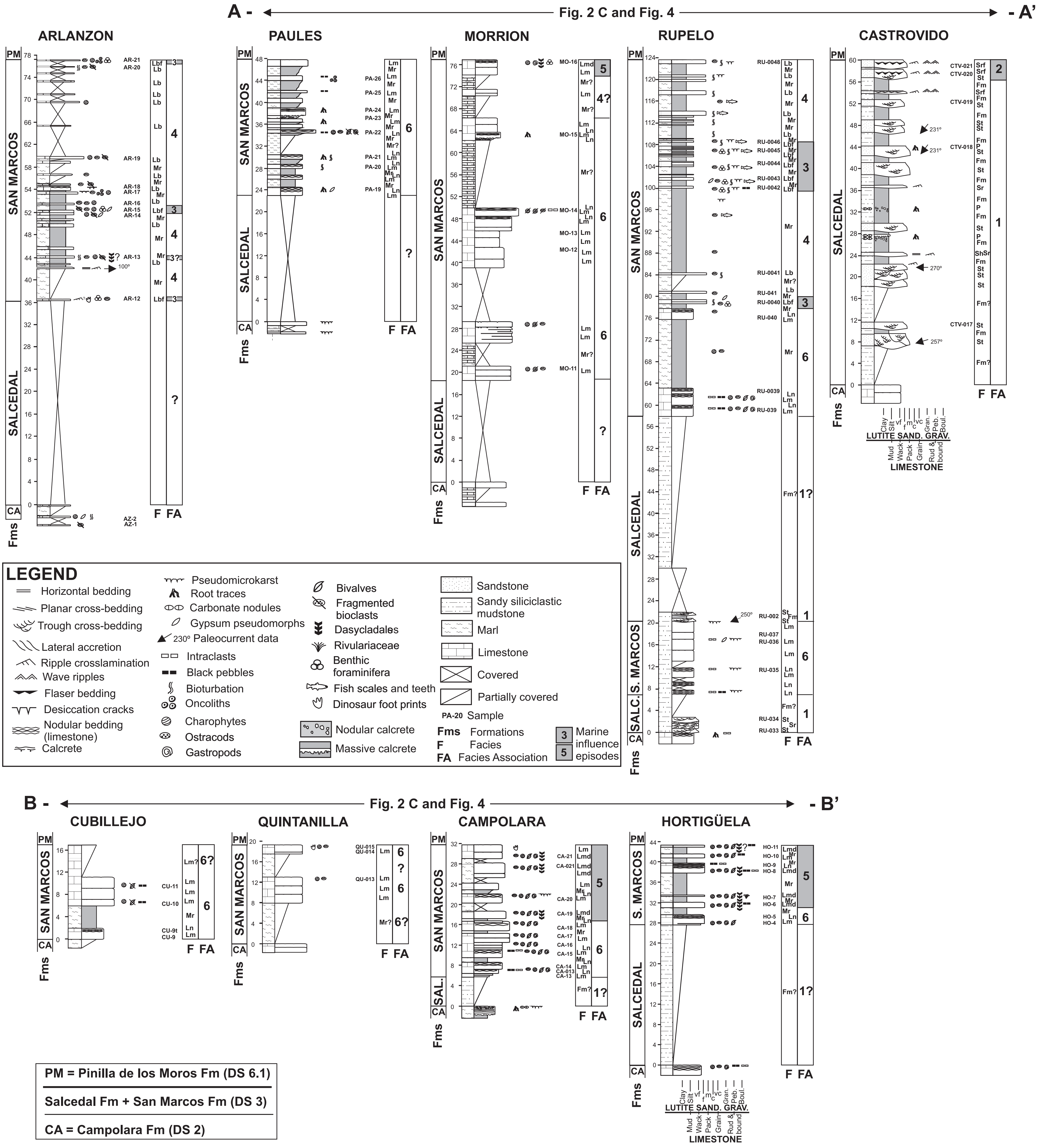

Figure
Click here to access/download;Figure;Fig_07_Mas-et-al_JIG_PDF.pdf

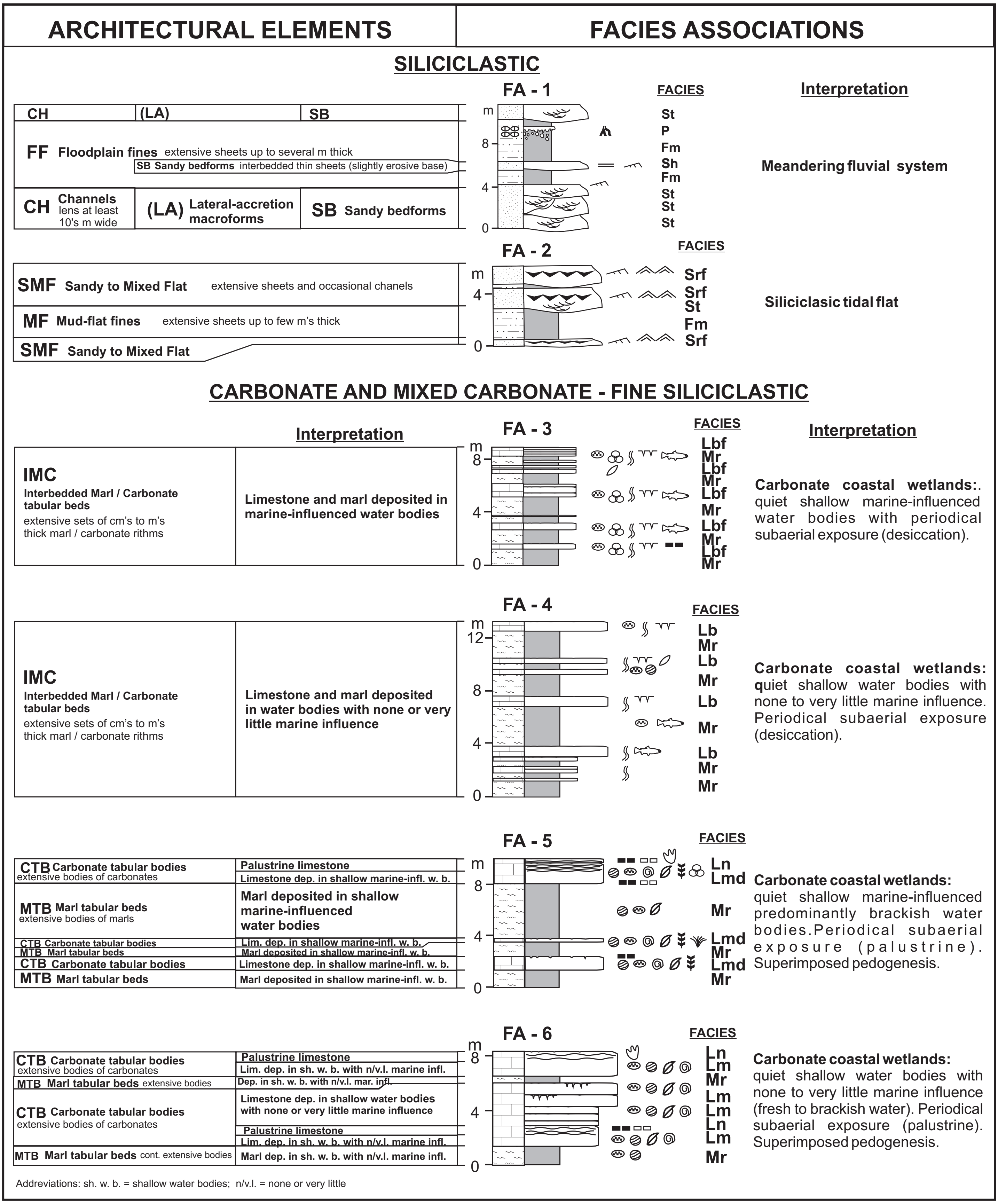

Figure

Click here to access/download;Figure;Fig_08_Mas-et-al_JIG_PDF.pdf

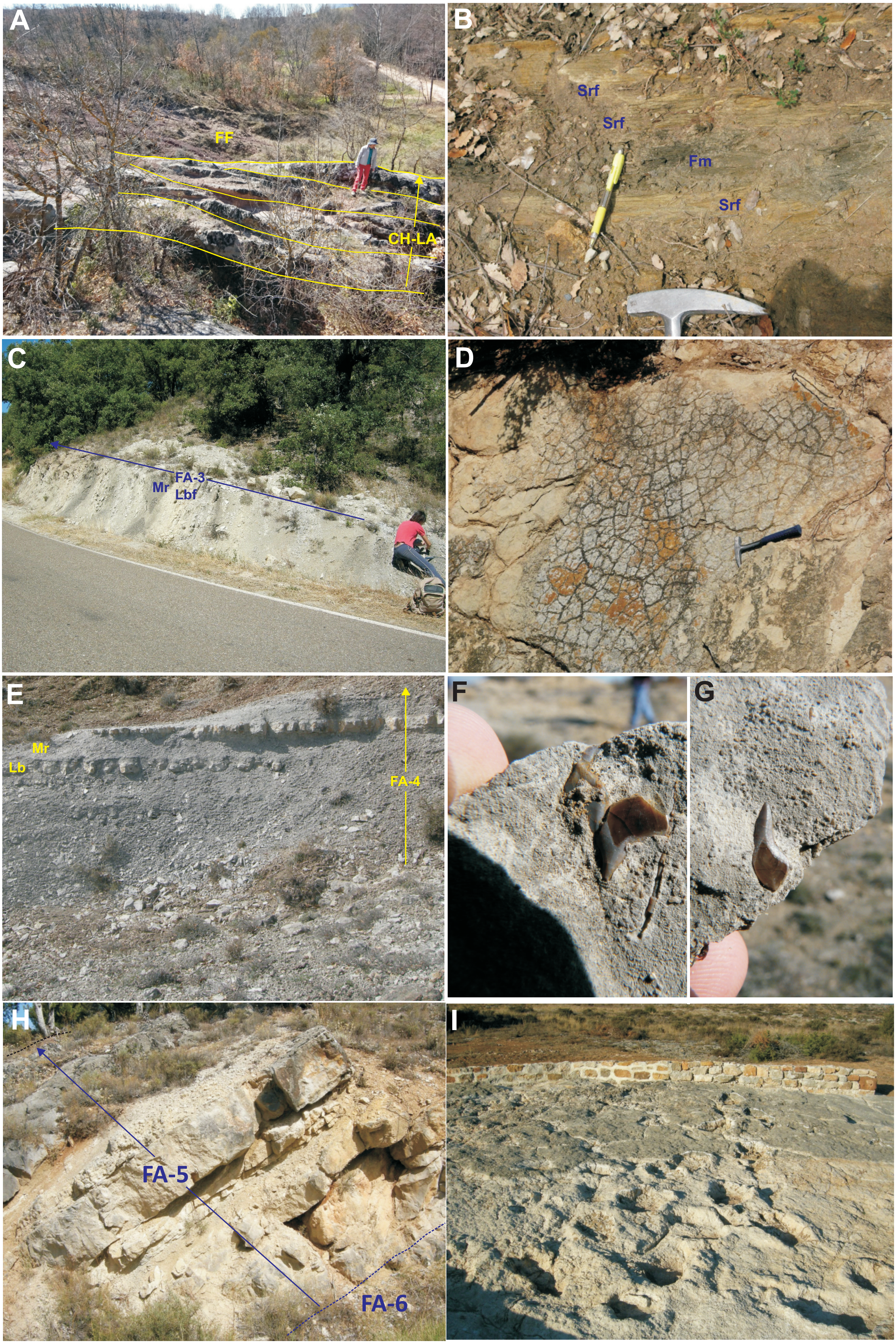

Click here to access/download;Figure;Fig_09_Mas-et-al_JIG_PDF.pdf

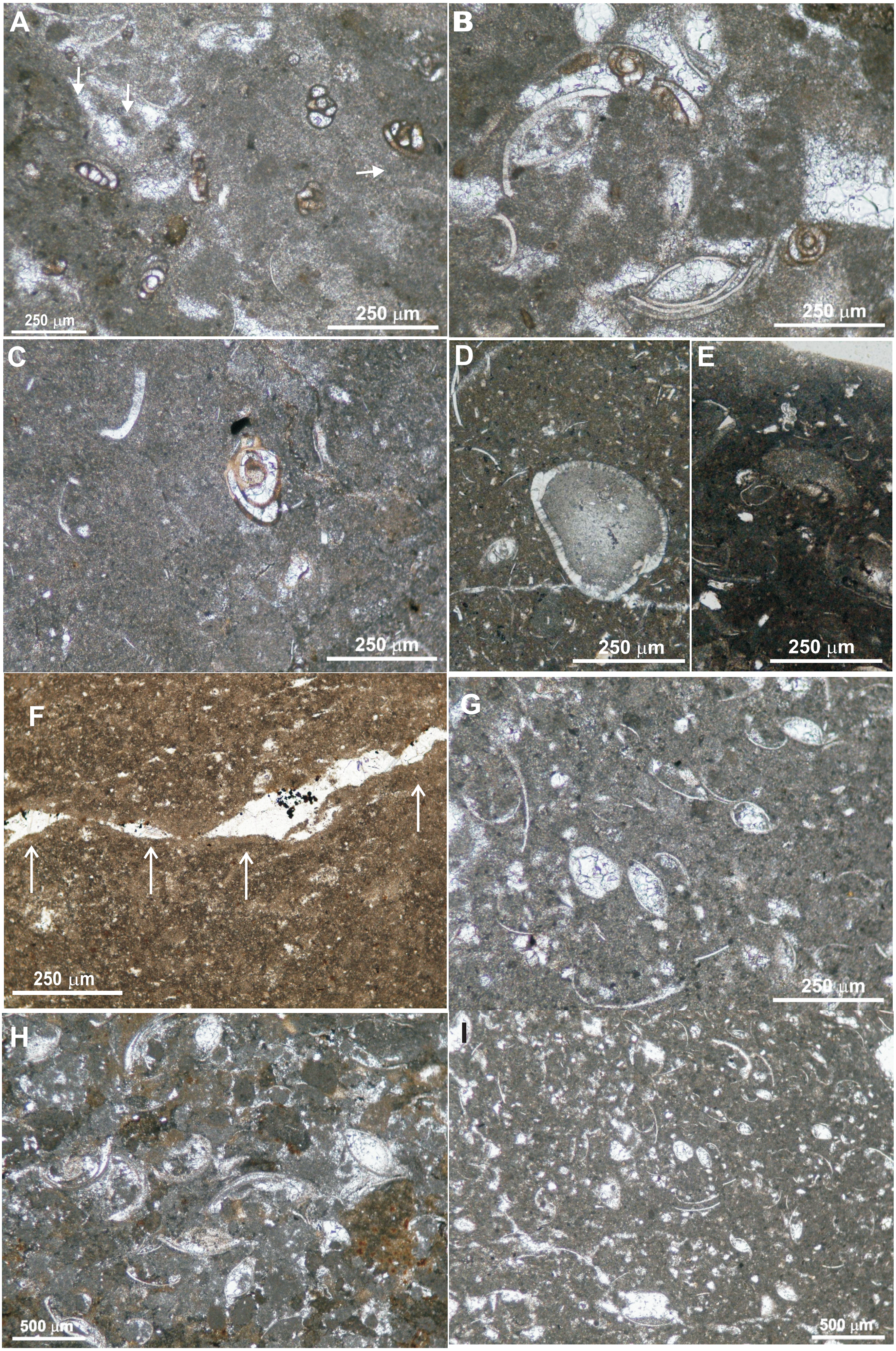

Figure

Click here to access/download;Figure;Fig_10_Mas-et-al_JIG_PDF.pdf

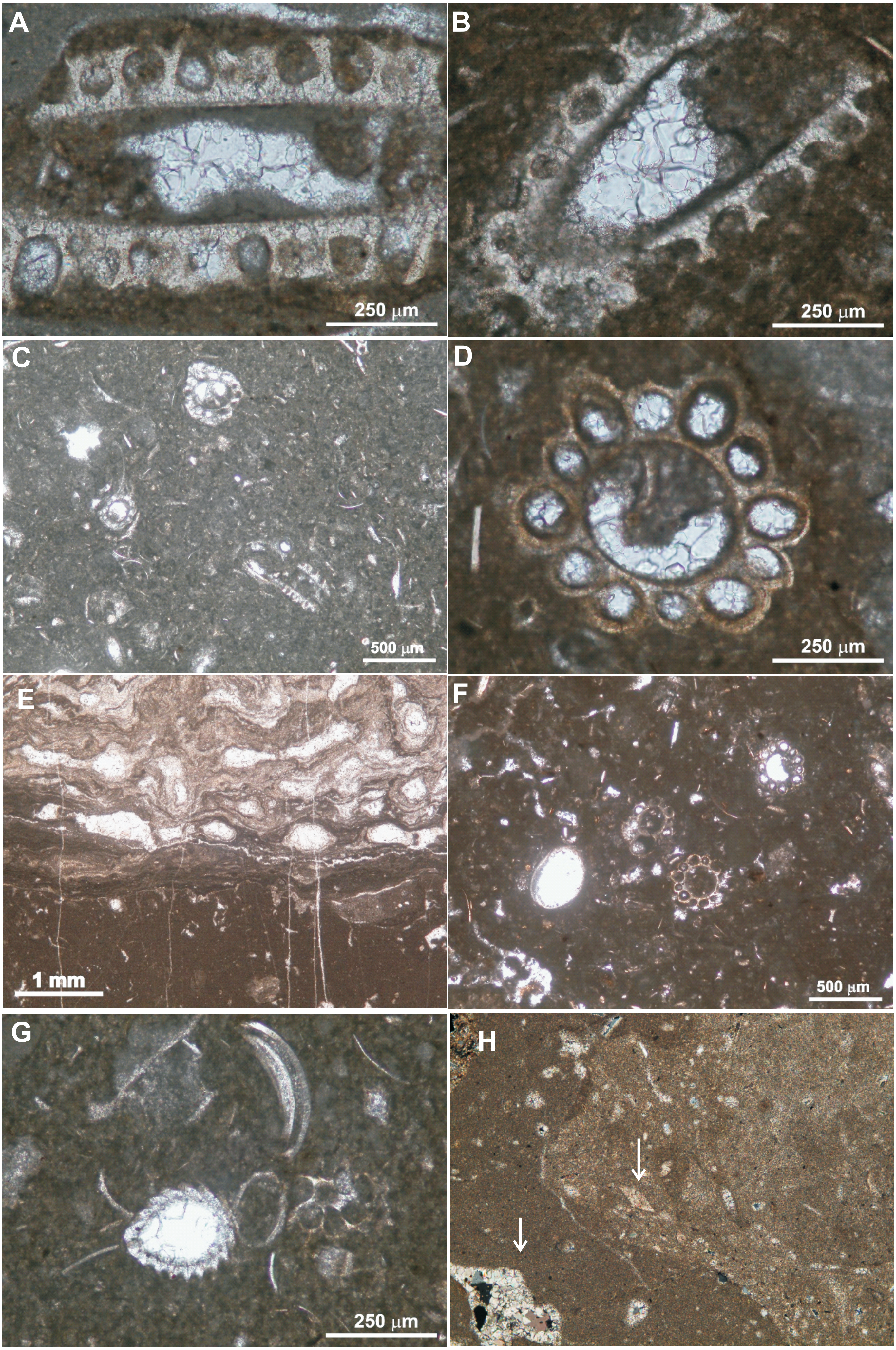

Figure
Click here to access/download;Figure;Fig_11_Mas-et-al_JIG_PDF.pdf

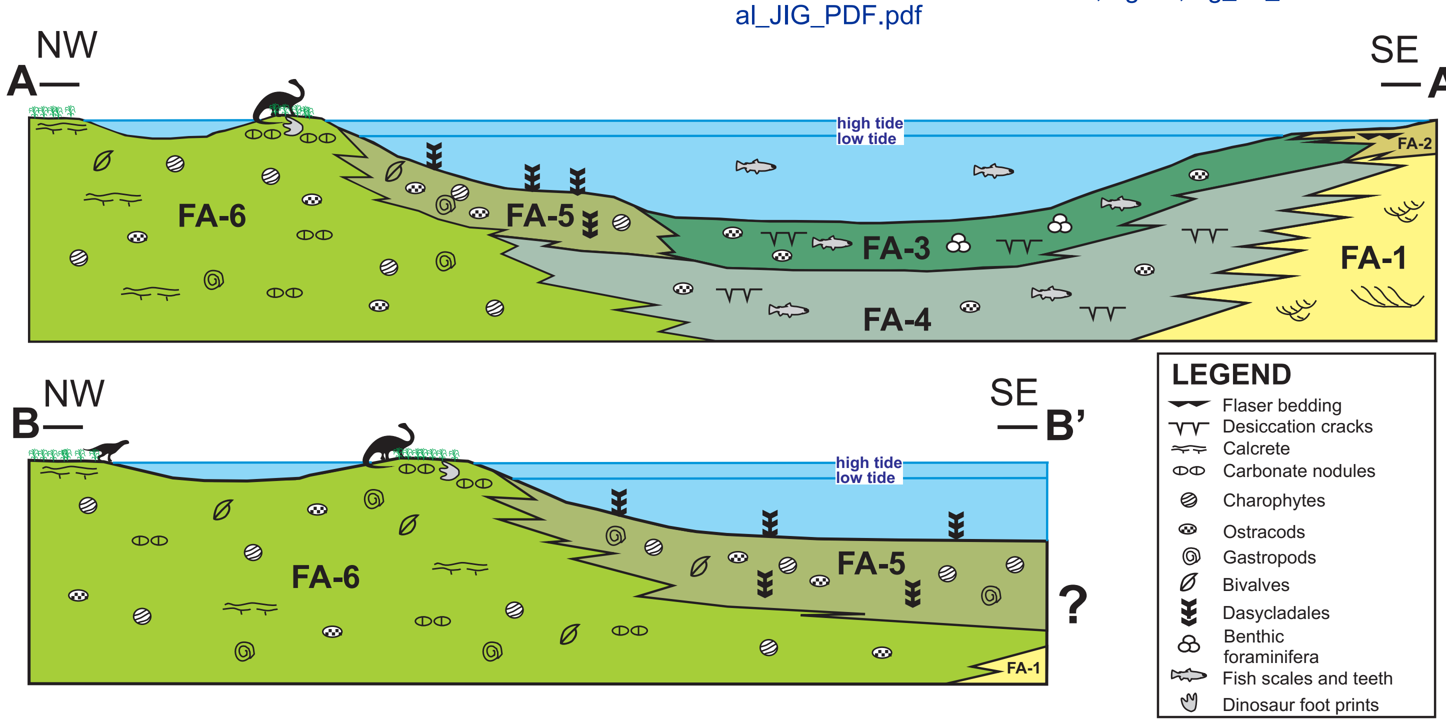

<table>
<tr><th>FACIES ASSOCIATIONS (Figs. 6 and 7)</th><th colspan="2">DEPOSITIONAL ENVIRONMENTS</th></tr>
<tr><td>FA-1</td><td colspan="2">Fluvial meandering</td></tr>
<tr><td>FA-2</td><td colspan="2">Siliciclastic tidal flat</td></tr>
<tr><td>FA-3</td><td>Shallow carbonate water bodies with marine influence and fine siliciclastic input</td><td rowspan="4">Carbonate coastal wetlands</td></tr>
<tr><td>FA-4</td><td>Shallow carbonate water bodies with none to very little marine influence and fine siliciclastic input</td></tr>
<tr><td>FA-5</td><td>Shallow carbonate water bodies with marine influence</td></tr>
<tr><td>FA-6</td><td>Shallow carbonate water bodies with none to very little marine influence and palustrine areas</td></tr>
</table>

Figure

Click here to access/download;Figure;Fig_12_Mas-et-al_JIG_PDF.pdf

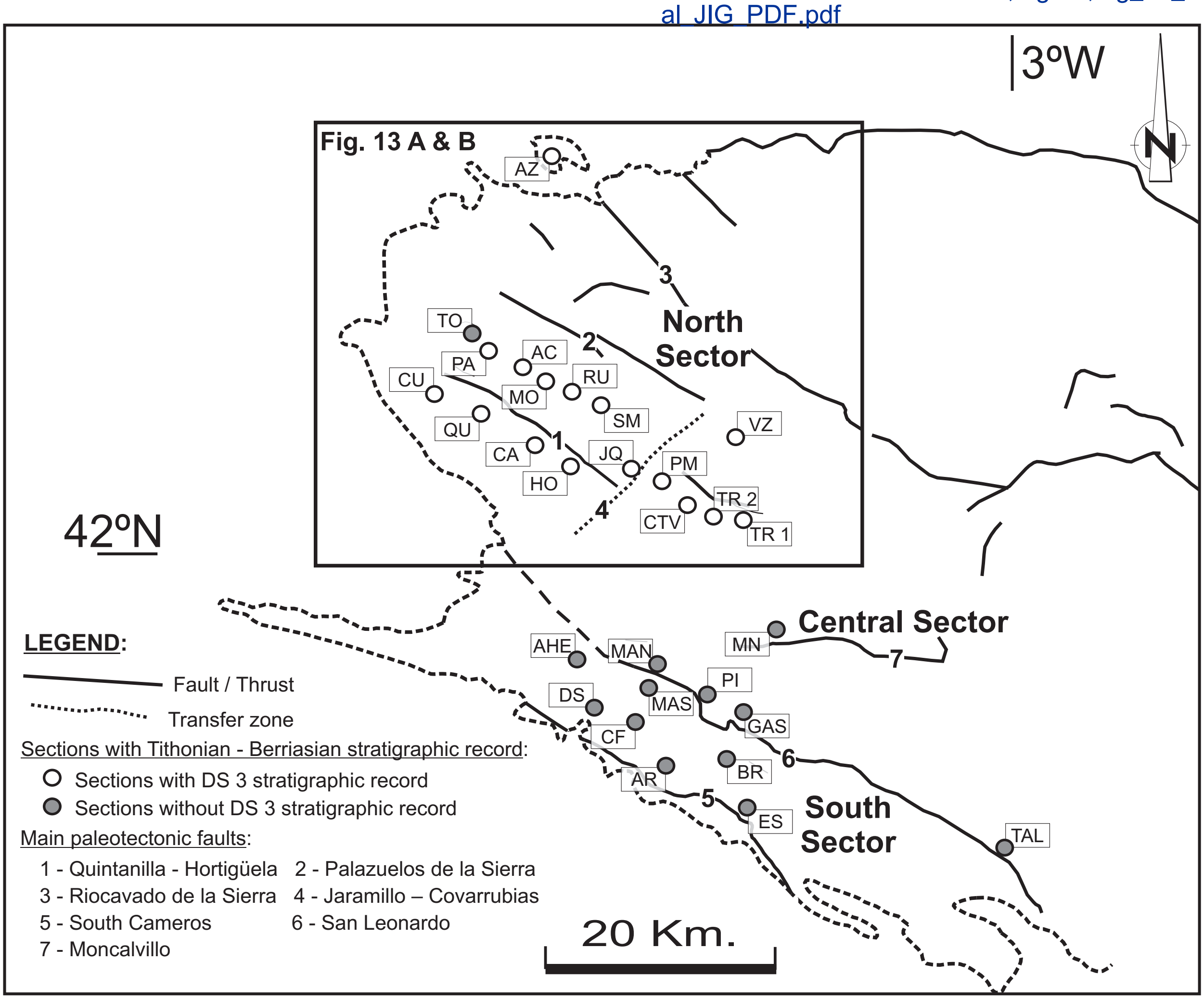

Figure

Click here to access/download;Figure;Fig_13_Mas-et-

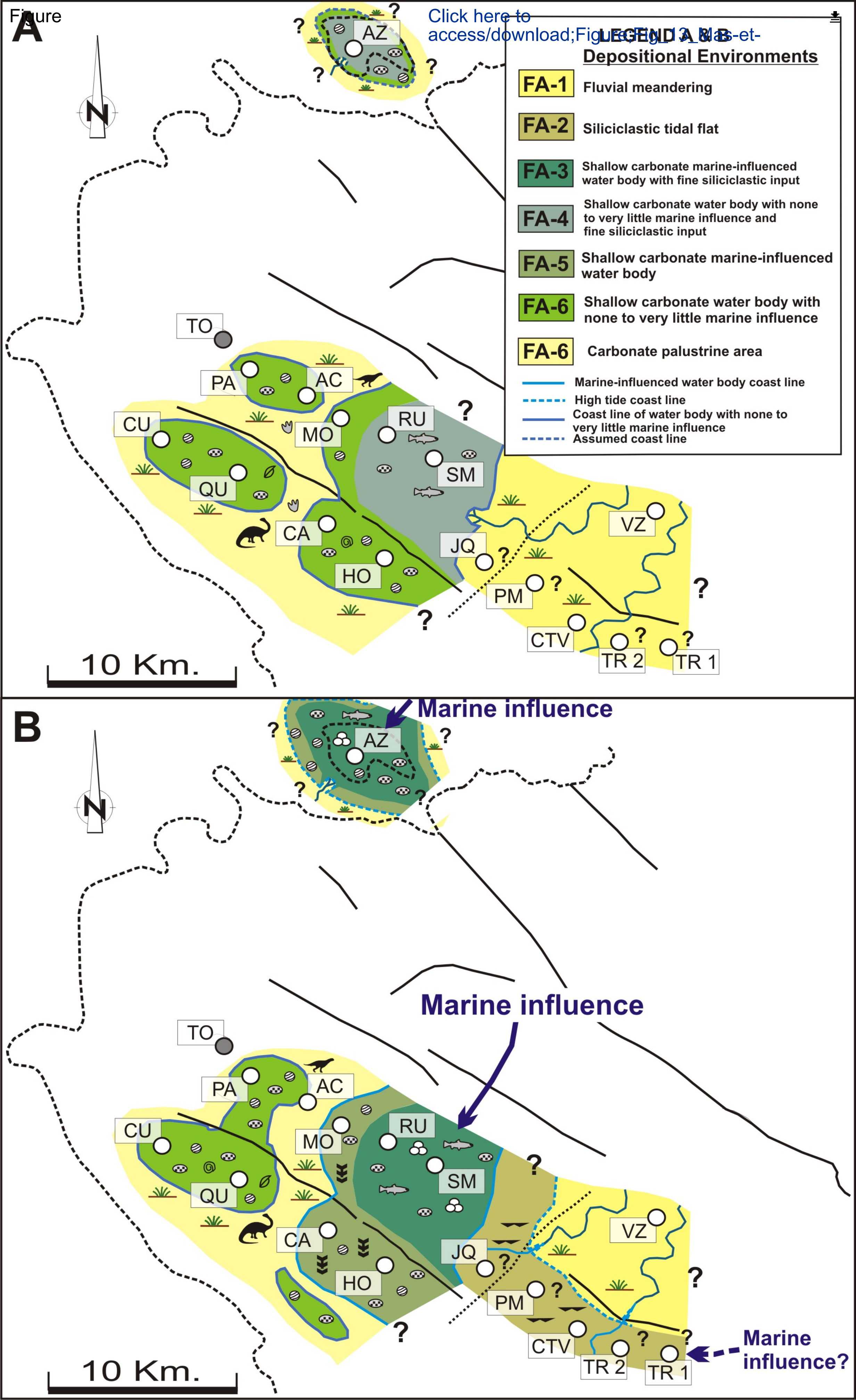

Figure

Click here to access/download;Figure;Fig_14_Mas-et-al_JIG_REV.pdf

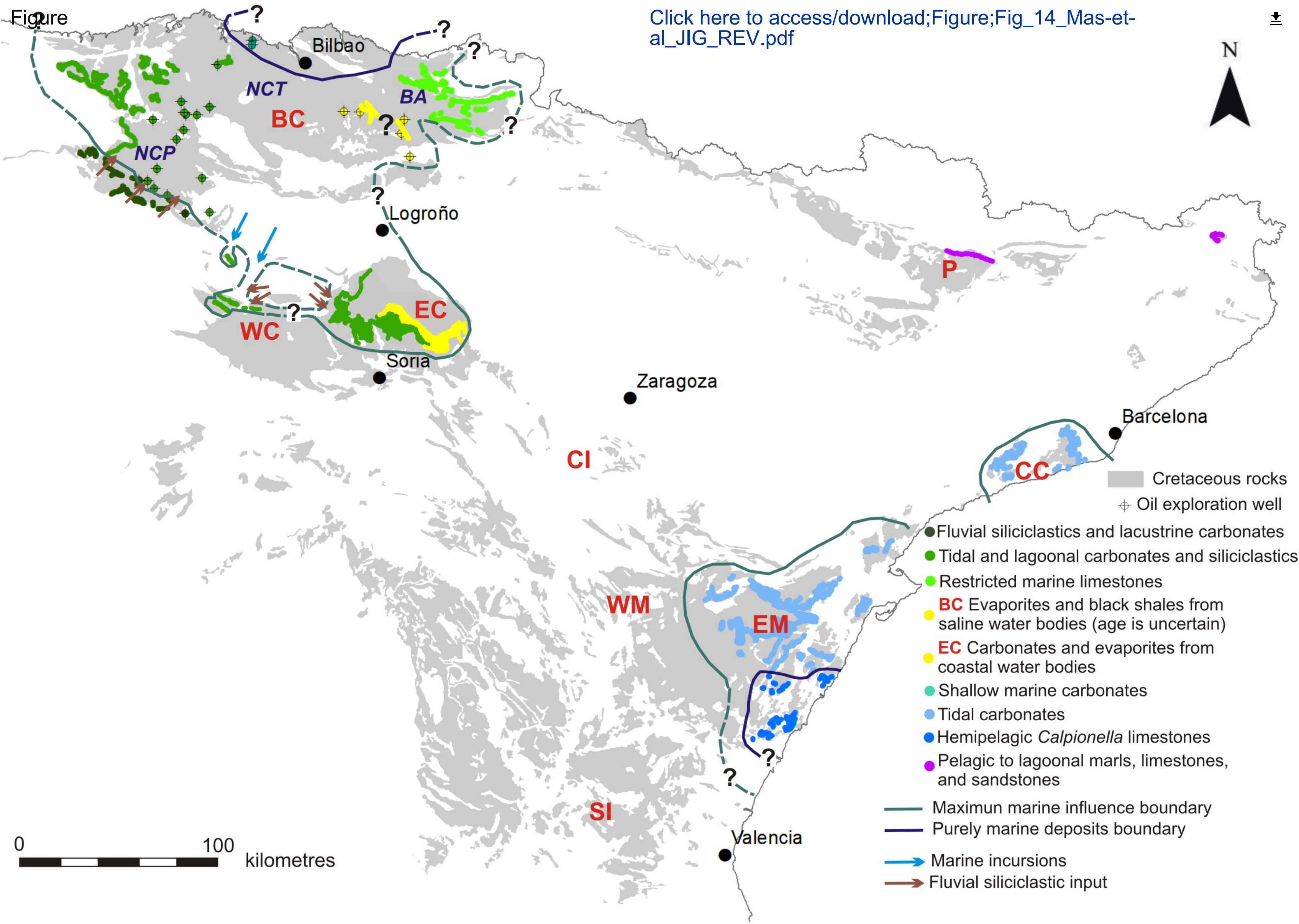

Figure
Click here to access/download;Figure;Fig_15_Mas-et-al_JIG_PDF.pdf